

A NUMERICAL STUDY OF AN IDEALIZED
OCEAN USING NON LINEAR LATERAL EDDY
VISCOSITY COEFFICIENTS

Julian Maynard Wright

Library
Naval Postgraduate School
Monterey, California 93944

NAVAL POSTGRADUATE SCHOOL

Monterey, California



THESIS

A NUMERICAL STUDY OF AN IDEALIZED OCEAN
USING NON LINEAR LATERAL EDDY VISCOSITY
COEFFICIENTS

by

Julian Maynard Wright, Jr.

March 1975

Thesis Advisor:

Robert L. Haney

Approved for public release; distribution unlimited.

T167580

REPORT DOCUMENTATION PAGE		READ INSTRUCTIONS BEFORE COMPLETING FORM
1. REPORT NUMBER	2. GOVT ACCESSION NO.	3. RECIPIENT'S CATALOG NUMBER
4. TITLE (and Subtitle) A Numerical Study of an Idealized Ocean Using Non Linear Lateral Eddy Viscosity Coefficients.		5. TYPE OF REPORT & PERIOD COVERED Master's Thesis; March 1975
		6. PERFORMING ORG. REPORT NUMBER
7. AUTHOR(s) Julian Maynard Wright, Jr.		8. CONTRACT OR GRANT NUMBER(s)
9. PERFORMING ORGANIZATION NAME AND ADDRESS Naval Postgraduate School Monterey, California 93940		10. PROGRAM ELEMENT, PROJECT, TASK AREA & WORK UNIT NUMBERS
11. CONTROLLING OFFICE NAME AND ADDRESS Naval Postgraduate School Monterey, California 93940		12. REPORT DATE March 1975
		13. NUMBER OF PAGES
14. MONITORING AGENCY NAME & ADDRESS (if different from Controlling Office) Naval Postgraduate School Monterey, California 93940		15. SECURITY CLASS. (of this report) Unclassified
		15a. DECLASSIFICATION/DOWNGRADING SCHEDULE
16. DISTRIBUTION STATEMENT (of this Report) Approved for public release; distribution unlimited.		
17. DISTRIBUTION STATEMENT (of the abstract entered in Block 20, if different from Report)		
18. SUPPLEMENTARY NOTES		
19. KEY WORDS (Continue on reverse side if necessary and identify by block number) eddy viscosity barotropic ocean model space computational oscillation non linear eddy viscosity wind driven ocean circulation		
20. ABSTRACT (Continue on reverse side if necessary and identify by block number) Using a one level, barotropic ocean model, driven by surface winds, a finite difference form of the vorticity equation was integrated over 210 days of simulated time. The solutions using constant coefficients of lateral eddy viscosity were compared with those using variable coefficients derived from enstrophy cascade and energy cascade. Using a constant eddy viscosity		

coefficient of rather low magnitude produces a large amplitude computational oscillation which fills the entire basin. An order of magnitude larger coefficient produces a marginally satisfactory solution, where the western boundary current was rather well represented, but a moderate computational oscillation was still evident. By increasing the coefficient yet another order of magnitude, the computational oscillation is negligible, but the solution in the ocean interior is unrealistically damped. An accurate physical and numerical depiction of both the ocean interior and western boundary with no computational oscillation was achieved by using either of the two forms of non linear eddy viscosity.

A Numerical Study of an Idealized Ocean Using
Non Linear Lateral Eddy Viscosity Coefficients

by

Julian Maynard Wright, Jr.
Lieutenant Commander, United States Navy
B.S., United States Naval Academy, 1963

Submitted in partial fulfillment of the
requirements for the degree of

MASTER OF SCIENCE IN METEOROLOGY

from the

NAVAL POSTGRADUATE SCHOOL
March 1975

ABSTRACT

Using a one level, barotropic ocean model, driven by surface winds, a finite difference form of the vorticity equation was integrated over 210 days of simulated time. The solutions using constant coefficients of lateral eddy viscosity were compared with those using variable coefficients derived from enstrophy cascade and energy cascade. Using a constant eddy viscosity coefficient of rather low magnitude produces a large amplitude computational oscillation which fills the entire basin. An order of magnitude larger coefficient produces a marginally satisfactory solution, where the western boundary current was rather well represented, but a moderate computational oscillation was still evident. By increasing the coefficient yet another order of magnitude, the computational oscillation is negligible, but the solution in the ocean interior is unrealistically damped. An accurate physical and numerical depiction of both the ocean interior and western boundary with no computational oscillation was achieved by using either of the two forms of non linear eddy viscosity.

TABLE OF CONTENTS

I.	INTRODUCTION-----	9
II.	THE MATHEMATICAL STATEMENT OF THE PROBLEM-----	12
	A. FORM OF THE VORTICITY EQUATION-----	12
	B. ENSTROPY CASCADE FORM OF NON LINEAR EDDY VISCOSITY-----	13
	C. KINETIC ENERGY CASCADE FORM OF NON LINEAR EDDY VISCOSITY-----	15
III.	THE MODEL AND FINITE DIFFERENCE EQUATIONS-----	18
	A. PHYSICAL CHARACTERISTICS OF THE MODEL-----	18
	B. FINITE DIFFERENCE FORM OF THE VORTICITY EQUATION-----	22
	1. Enstrophy Cascade Case-----	24
	2. Kinetic Energy Cascade Case-----	27
	3. Solution Description-----	29
IV.	RESULTS-----	31
	A. RESTATEMENT OF PURPOSE-----	31
	B. ANALYTICAL CONSIDERATIONS-----	31
	C. EXPERIMENTS WITH CONSTANT COEFFICIENTS OF EDDY VISCOSITY-----	32
	D. EXPERIMENTS WITH NON LINEAR COEFFICIENTS OF EDDY VISCOSITY-----	35
V.	CONCLUSIONS-----	61
	APPENDIX A: COMPUTER PROGRAM-----	62
	LIST OF REFERENCES-----	73
	INITIAL DISTRIBUTION LIST-----	74

LIST OF TABLES

I.	Summary of Results for Significant Numerical Experiments with Constant Coefficients of Lateral Eddy Viscosity A_1 , A_2 , and A_3 as Compared to Analytical Results-----	37
II.	Summary of Results for Significant Experiments with Non Linear Coefficient of Eddy Viscosity $AMIN = A_1 = .12 \times 10^8 \text{ cm}^2 \text{ sec}^{-1}$ -----	49
III.	Summary of Results for Significant Experiments with Non Linear Coefficients of Eddy Viscosity $AMIN = A_2$ and A_3 -----	58

LIST OF FIGURES

1.	The Staggered Grid with Corner Boundary-----	19
2.	Wind Stress Pattern-----	21
3.	Analytical Solutions of Ψ at Latitude with Maximum Streamfunction for A_1 , A_2 , and A_3 = Constants-----	33
4.	Numerical Solution of Streamfunction for A_1 = Constant-----	34
5.	Numerical Solution of Streamfunction for A_2 = Constant-----	36
6.	Numerical Solution of Streamfunction for A_3 = Constant-----	38
7.	Numerical and Analytical Solutions of Ψ at Latitude with Maximum Streamfunction for Non Linear Experiments with $A_1 \sim D $ -----	39
8.	Numerical Solutions of Ψ for A_1 and $m = 10$ A. Symmetric Boundary Conditions for $A \sim \nabla \zeta $ -----	41
	B. Extrapolated Boundary Conditions for $A \sim \nabla \zeta $ -----	43
	C. $A \sim D $ -----	44
9.	Numerical Solutions of Ψ for A_1 and $m = 100$ A. Symmetric Boundary Conditions for $A \sim \nabla \zeta $ -----	46
	B. Extrapolated Boundary Conditions for $A \sim \nabla \zeta $ -----	47
	C. $A \sim D $ -----	48
10.	Numerical Solutions of Ψ for A_1 and $m = 1000$ A. Symmetric Boundary Conditions for $A \sim \nabla \zeta $ -----	50
	B. Extrapolated Boundary Conditions for $A \sim \nabla \zeta $ -----	51
	C. $A \sim D $ -----	52
11.	Numerical and Analytical Solutions of Ψ at Latitude with Maximum Streamfunction for Non Linear Experiments with $A_2 \sim \nabla \zeta $ -----	54
12.	Numerical Solutions of Ψ for A_2 and $m = 10$ A. Extrapolated Boundary Conditions for A -----	55
	B. $A \sim D $ -----	56
13.	Numerical Solutions of Ψ for A_2 and $m = 21$, Extrapolated Boundary Conditions for A -----	57
14.	Numerical Solutions of Ψ for A_3 and $m = 10$, $A \sim D $ -----	60

ACKNOWLEDGEMENT

The author wishes to express his deep appreciation and thanks to Dr. Robert L. Haney, whose ceaseless encouragement and patience made possible the successful completion of this thesis project. Further, not enough thanks can be extended to my wife Anne and son Andrew for their unfailing support and understanding in this thesis project and throughout my tour at the Naval Postgraduate School.

I also extend my appreciation to Roland Sweet of NCAR for his fast and accurate Poisson solver subroutine and to Professor Frank Faulkner of the Naval Postgraduate School for his revision of it for this model. Computer time for the numerical calculations was provided by the W. R. Church Computer Center at the Naval Postgraduate School.

I. INTRODUCTION

This study is part of a broader effort to develop the capability of making large scale oceanographic predictions on a dynamical basis. The large-scale and meso-scale thermal structure of the ocean is very dynamic and is related to most marine and atmospheric processes. Some of the most obvious relationships to sea surface temperature (SST) are ocean fronts, circulation, currents, and sea state; and atmospheric temperature, circulation, and wind velocity. The effect that these environmental phenomena can have on naval and maritime operations is well known.

The significance of the long range effect of SST anomalies on weather patterns has received increasing scientific awareness. On 20 August 1974, J. Namias, at a NORPAX Conference at the U.S. Naval Postgraduate School, reported on the results of an empirical ocean/atmosphere prediction model. With a knowledge of SST anomalies in the spring of 1974, Namias derived fields of atmospheric temperature anomalies and circulation for the following summer. Namias predicted in May that a comparatively severe drought would occur over the midwestern United States during the summer of 1974. Later events verified his forecast.

One of the areas of difficulty in adequately representing the circulation and anomalies in a finite-grid ocean circulation model, and subsequently satisfying and integrating the

equations of motion, is the representation of internal frictional effects within the ocean fluid.

Using linear theory, Takano [1974] showed that if the coefficient of eddy viscosity is too small, a computational oscillation in space results from not resolving the western boundary current. This computational oscillation fills the entire basin and contaminates the solution. On the other hand, if the coefficient is increased, the open ocean solution is too viscous. To handle this problem, Takano showed that the use of upstream differencing in the beta term of the vorticity equation allows a smaller coefficient than permitted by linear theory. However, this method unfortunately produces excessive damping of time dependent motion. In addition, this mathematical scheme is not representative of any physical motion in the ocean. A better approach, from a physical point of view, is the use of non linear eddy viscosity. The friction force which arises using non linear eddy viscosity is extremely sensitive to the scale of the motion, and therefore will be relatively small in the oceans' interior where the scales are comparatively large, and will be relatively large in the western boundary region where the scales are comparatively small. The comparatively large dissipation in the western boundary region will keep the current broad enough to be resolved by the grid and thereby prevent the formation of any computational oscillation.

In 1968, Leith examined two dimensional turbulence advection and derived non linear coefficients of eddy

viscosity from the cascade of enstrophy from large scale to small scale motion. In this case, the coefficient of eddy viscosity is proportional to the magnitude of the horizontal gradient of vorticity.

Another satisfactory non linear procedure was introduced by Smagorinsky [1963] in which an estimate of the energy cascade rate is made from the fluid deformation itself. In this case, the coefficient of eddy viscosity is proportional to the absolute value of the deformation.

The purpose of this thesis is to introduce non linear coefficients of lateral eddy viscosity that are not only reasonably representative of actual physical conditions, but these same coefficients must retain their reasonable representation when used in finite grid numerical ocean circulation models. In addition, with these coefficients the numerical model must remain computationally stable in long term integration. Integrations using both of the above forms of non linear eddy viscosity are examined and compared with numerical and analytic results using constant coefficients.

II. THE MATHEMATICAL STATEMENT OF THE PROBLEM

A. FORM OF THE VORTICITY EQUATION

The continuity equation for a homogeneous fluid and the non linear equations of horizontal motion, cross differentiated to eliminate the pressure term, form the basis for the vorticity equation:

$$\frac{d\zeta}{dt} + v\beta + f\nabla \cdot \mathbf{V} = \frac{\partial}{\partial x}(F_y + \frac{\tau_y}{\rho_0 H}) - \frac{\partial}{\partial y}(F_x + \frac{\tau_x}{\rho_0 H})$$

$$\text{or } \frac{\partial \zeta}{\partial t} + \mathbf{V} \cdot \nabla \zeta + v\beta + f\nabla \cdot \mathbf{V} = \frac{\partial}{\partial x}(F_y + \frac{\tau_y}{\rho_0 H}) - \frac{\partial}{\partial y}(F_x + \frac{\tau_x}{\rho_0 H}) \quad (\text{II-1})$$

where $\beta = \frac{df}{dy}$ is taken constant. In (II-1), (τ_x, τ_y) is the surface stress, H is the constant basin depth, and all other symbols have their usual meaning. Bottom stress was neglected.

The friction forces are represented by

$$F_x = \nabla \cdot (A \nabla u)$$

$$F_y = \nabla \cdot (A \nabla v) \quad (\text{II-2})$$

where A is the coefficient of lateral eddy viscosity and (u, v) is the vertically averaged velocity, as discussed below.

The model is designed with a "rigid surface," in order to filter gravity waves from the system:

$$w(0) = 0.$$

It is also necessary that there be no vertical motion on the flat ocean floor:

$$w(-H) = 0.$$

Because w is zero at the top and bottom, the divergence of

the vertically averaged current, \bar{V} , is zero.

$$\nabla \cdot \bar{V} = 0.$$

Therefore \bar{V} can be defined by a streamfunction, ψ ,

$$\bar{u} = - \frac{\partial \psi}{\partial y}$$

$$\bar{v} = \frac{\partial \psi}{\partial x}.$$

Integrating (II-1) from top to bottom and using $\nabla \cdot \bar{V} = 0$, the final form of the vertically integrated vorticity equation was written

$$\begin{aligned} \frac{\partial}{\partial t} \nabla^2 \psi + \beta \frac{\partial \psi}{\partial x} = & \frac{\partial}{\partial x} (-\bar{V} \cdot \nabla \bar{v} + F_y + \frac{\tau_y}{\rho_0 H}) \\ & - \frac{\partial}{\partial y} (-\bar{V} \cdot \nabla \bar{u} + F_x + \frac{\tau_x}{\rho_0 H}) \end{aligned} \quad (\text{II-3})$$

Equation (II-3) also includes the assumption that

$$\overline{V \cdot \nabla V} = \bar{V} \cdot \bar{\nabla}, \text{ etc.}$$

The next section will discuss the formulation of the friction terms, F_x and F_y , which depend upon the non linear eddy viscosity coefficient, A .

B.. ENSTROPY CASCADE FORM OF NON LINEAR EDDY VISCOSITY

The first method of generating non linear coefficients of eddy viscosity is through the theory of two dimensional turbulence, in which enstrophy and kinetic energy are conserved by the advective terms. Using these principles, Kraichman [1967] and Leith [1968] derived the relation

$$E(k) \propto \eta^{2/3} k^{-3} \quad (\text{II-4})$$

where η is the assumed constant cascading rate of mean squared vorticity and $E(k)$ is the kinetic energy in wave number k .

The eddy viscosity which causes the dissipation is also assumed

a function of η and k , and by dimensional analysis

$$A = \alpha \eta^{1/3} k^{-2} \quad (\text{II-5})$$

where α is a constant.

One estimate of η made locally as a function of surrounding data was made by Leith

$$\eta = A(\nabla \zeta) \cdot (\nabla \zeta) = A|\nabla \zeta|^2, \quad (\text{II-6})$$

where ζ is the local vertical component of vorticity.

Substituting (II-6) into (II-5) and solving for A leads to

$$A = (\alpha^{1/2}/k)^3 |\nabla \zeta|.$$

Assuming that the wave number $k_* = 2\pi/d$, where d is the grid size, lies in the inertial subrange, the final form of non linear eddy viscosity for enstrophy cascade becomes

$$A = (\alpha^{1/2} \frac{d}{2\pi})^3 |\nabla \zeta|. \quad (\text{II-7})$$

Denoting the minimum viscosity coefficient by A_0 , the viscosity in the model was written,

$$A = A_0 + \gamma |\nabla \zeta| d^3 \quad (\text{II-8})$$

A is a maximum when $|\nabla \zeta|$ is maximum. Defining $A_{\max} = mA_0$, then (II-8) becomes

$$A_{\max} = mA_0 = A_0 + \gamma |\nabla \zeta|_{\max} d^3 \quad (\text{II-9})$$

Solving for γ

$$\gamma = \frac{A_0(m-1)}{|\nabla \zeta|_{\max} d^3} \quad (\text{II-10})$$

The quantity $|\nabla \zeta|_{\max}$ was estimated by

$$|\nabla \zeta|_{\max} = 6.67 \times 10^{-14} \text{ cm}^{-1} \text{ sec}^{-1} \quad (\text{II-11})$$

which for $d = 300 \text{ km}$ leads to a value for γ of

$$\gamma = \frac{A_0(m-1)}{1.8 \times 10^9} \quad (\text{II-12})$$

Substituting this into (II-8) gives the final equation for the enstrophy cascade form of non linear eddy viscosity for this study:

$$A = A_0 \left(1 + \frac{(m-1) |\nabla \zeta|}{|\nabla \zeta|_{\max}} \right) = A_0 \left(1 + \frac{(m-1) |\nabla \zeta|}{6.67 \times 10^{-1}} \right) \quad (\text{II-13})$$

In (II-13), Ψ_{\max} was taken from linear theory [Munk, 1950], and m was considered an adjustable parameter.

With this non linear form of eddy viscosity, the vertically averaged friction force terms in the x and y directions become from (II-2)

$$F_x = \frac{\partial}{\partial x} \left(A \frac{\partial \bar{u}}{\partial x} \right) + \frac{\partial}{\partial y} \left(A \frac{\partial \bar{u}}{\partial y} \right) \quad (\text{II-14})$$

$$F_y = \frac{\partial}{\partial x} \left(A \frac{\partial \bar{v}}{\partial x} \right) + \frac{\partial}{\partial y} \left(A \frac{\partial \bar{v}}{\partial y} \right) . \quad (\text{II-15})$$

The vertical component of the curl of the friction force becomes

$$\text{CURL}_z F = \frac{\partial F_y}{\partial x} - \frac{\partial F_x}{\partial y} . \quad (\text{II-16})$$

C. KINETIC ENERGY CASCADE FORM OF NON LINEAR EDDY VISCOSITY

From dimensional arguments, Leith [1968] showed that in three dimensional turbulence, if the energy cascade rate from large scale to small scale is proportional only to kinetic energy dissipation (ϵ) and wave number (k), then

$$E(k) = \alpha_1 \epsilon^{2/3} k^{-5/3} . \quad (\text{II-17})$$

If, in addition to this equation, it is assumed that eddy viscosity, which produces the dissipation, is also a function of ϵ and k only, then by dimensional arguments

$$A = \alpha_2 \epsilon^{1/3} k^{-4/3} \quad (\text{II-18})$$

where k lies in an inertial subrange. Assuming the dissipation rate is constant, then $k^{-4/3} \sim d^{4/3}$. This quasi-linear eddy viscosity is dependent only on grid size, and hence latitude if the grid size is latitude dependent. But more realistically, dissipation is not constant nor independent of motion or grid size. Smagorinsky [1963] assumes a local value of dissipation:

$$\epsilon = A |D|^2 \quad (\text{II-19})$$

where $|D|$ is the magnitude of the deformation tensor. In this case (II-18) becomes

$$A = \alpha_2^{3/2} |D| d^2 \quad (\text{II-20})$$

In the deformation tensor $|D| = \sqrt{D_s^2 + D_t^2}$, the shearing deformation is $D_s = \frac{\partial v}{\partial x} + \frac{\partial u}{\partial y}$ and stretching deformation is $D_t = \frac{\partial u}{\partial x} - \frac{\partial v}{\partial y}$.

The Smagorinsky equation takes the form similar to (II-8) for this study

$$A = A_0 + \gamma |D| d^2. \quad (\text{II-21})$$

Defining $A_{\max} = mA_0$, equation (II-21) becomes

$$mA_0 = A_0 + \gamma |D|_{\max} d^2 \quad (\text{II-22})$$

Solving for γ

$$\gamma = \frac{A_0(m-1)}{|D|_{\max} d^2}. \quad (\text{II-23})$$

Using (II-23) in II-21), the final energy cascade form of the non linear eddy viscosity becomes

$$A = A_0 \left[1 + \frac{(m-1)}{\left| \frac{D}{D} \right|_{\max}} \right] \quad (\text{II-24})$$

The form of the friction force principally used in the model for the kinetic energy cascade case was of the form of (II-14) and (II-15). Experiments following the friction force of Smagorinsky [1963] were also used for comparison:

$$F_x = \frac{\partial}{\partial x} (A D_t) + \frac{\partial}{\partial y} (A D_s) \quad (\text{II-25})$$

$$F_y = \frac{\partial}{\partial x} (A D_s) - \frac{\partial}{\partial y} (A D_t) \quad (\text{II-26})$$

In both cases the curl of the friction force term was (II-16).

III. THE MODEL AND FINITE DIFFERENCE EQUATIONS

A. PHYSICAL CHARACTERISTICS OF THE MODEL

The model consisted of a one-level barotropic ocean in a square basin of length, $L = 9600$ km; of breadth, $B = 9600$ km; and a flat bottom of constant depth, $H = 2$ km. A portion of the staggered grid is shown in Figure 1. The total grid points (excluding the boundary buffer) are 33×33 , and the distance between adjacent grid points is

$$X = Y = d = 300 \text{ km.} \quad (\text{III-1})$$

The value chosen for β corresponds to a grid centered at 32.5° N.

The staggered grid consists primarily of: 1) the intersections, or principal grid points (\cdot), where are defined the streamfunction (Ψ), vorticity (ζ), deformation (D), and the coefficient of eddy viscosity (A_D) generated from deformation; and 2) the grid centers (o), where are defined velocity (u, v), the gradient of vorticity ($\nabla \zeta$), the friction force (F_x, F_y), and the coefficient of eddy viscosity (A_ζ) generated from ($\nabla \zeta$). Auxiliary variables were defined at cross (x) points.

The model is not strictly designed to simulate any particular ocean, but rather to be representative of the fundamental physical characteristics of mass transport and western boundary current of an ocean in the northern hemisphere as affected by the viscous action of the ocean's large scale circulation.

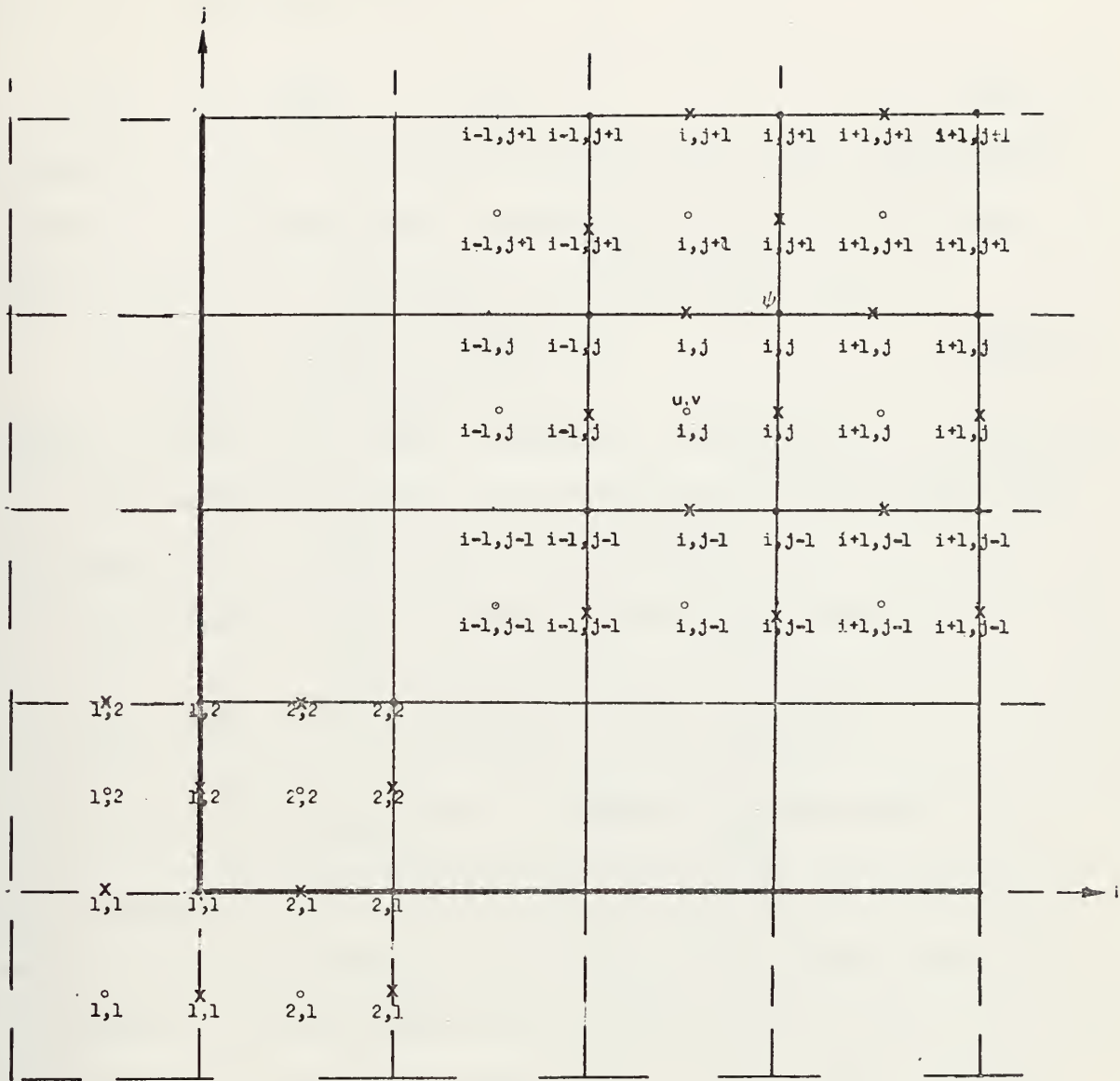


Figure 1: The Staggered Grid with Corner Boundary. The solid line represents the physical boundary of the basin.

- (•) Principal grid point (ψ , ζ , D , $A(|D|)$)
- (o) Grid center (u , v , $\nabla \zeta$, $A(\nabla \zeta)$, F_x , F_y)
- (x) Grid average points (U_{AV} , V_{AV} , U_{AVE} , V_{AVE} , $A(|D|)_{ave}$, $F_{x\ ave}$, $F_{y\ ave}$)

The energy for this barotropic wind driven circulation model is represented by

$$\frac{\tau_x}{\rho_0} = -F \cos\left(\frac{2ny}{B}\right), \quad \tau_y = 0, \quad (\text{III-2})$$

a pattern of westerly winds in the center half and easterly winds in the northern and southern quarters of the ocean (See Figure 2). This leads to a stress curl term

$$-\frac{\partial}{\partial y}\left(\frac{\tau_x}{\rho_0 H}\right)_j = -\frac{2nf}{HB} \sin\left(\frac{2ny_j}{B}\right) \Delta x^2, \quad (\text{III-3})$$

which provides the actual forcing in the vorticity equation. F is the amplitude of the zonal component of the wind, and B is the north-south extent of the domain.

The velocity (u,v) written in numerical form is

$$u_{i,j} = \frac{1}{d} \left[\frac{(\psi_{i-1,j-1} + \psi_{i,j-1})}{2} - \frac{(\psi_{i-1,j} + \psi_{i,j})}{2} \right]$$

$$v_{i,j} = \left[\frac{(\psi_{i,j} + \psi_{i,j-1})}{2} - \frac{(\psi_{i-1,j} + \psi_{i-1,j-1})}{2} \right]$$

The boundary conditions for (u,v) used along the coastline were zero normal flow and zero slip. Zero normal flow was attained by requiring the streamfunction (ψ) on the left side of equation (II-3) to be equal zero on the ocean perimeter. To implement the condition of zero normal flow and zero slip in the terms on the right hand side of (II-3), the velocity is defined as zero on the coastline by defining the zonal boundaries

$$\begin{aligned} u_{i,1} &= -u_{i,2} & u_{i,34} &= -u_{i,33} \\ v_{i,1} &= -v_{i,2} & v_{i,34} &= -v_{i,33}, \end{aligned} \quad (\text{III-5})$$

for the meridional boundaries

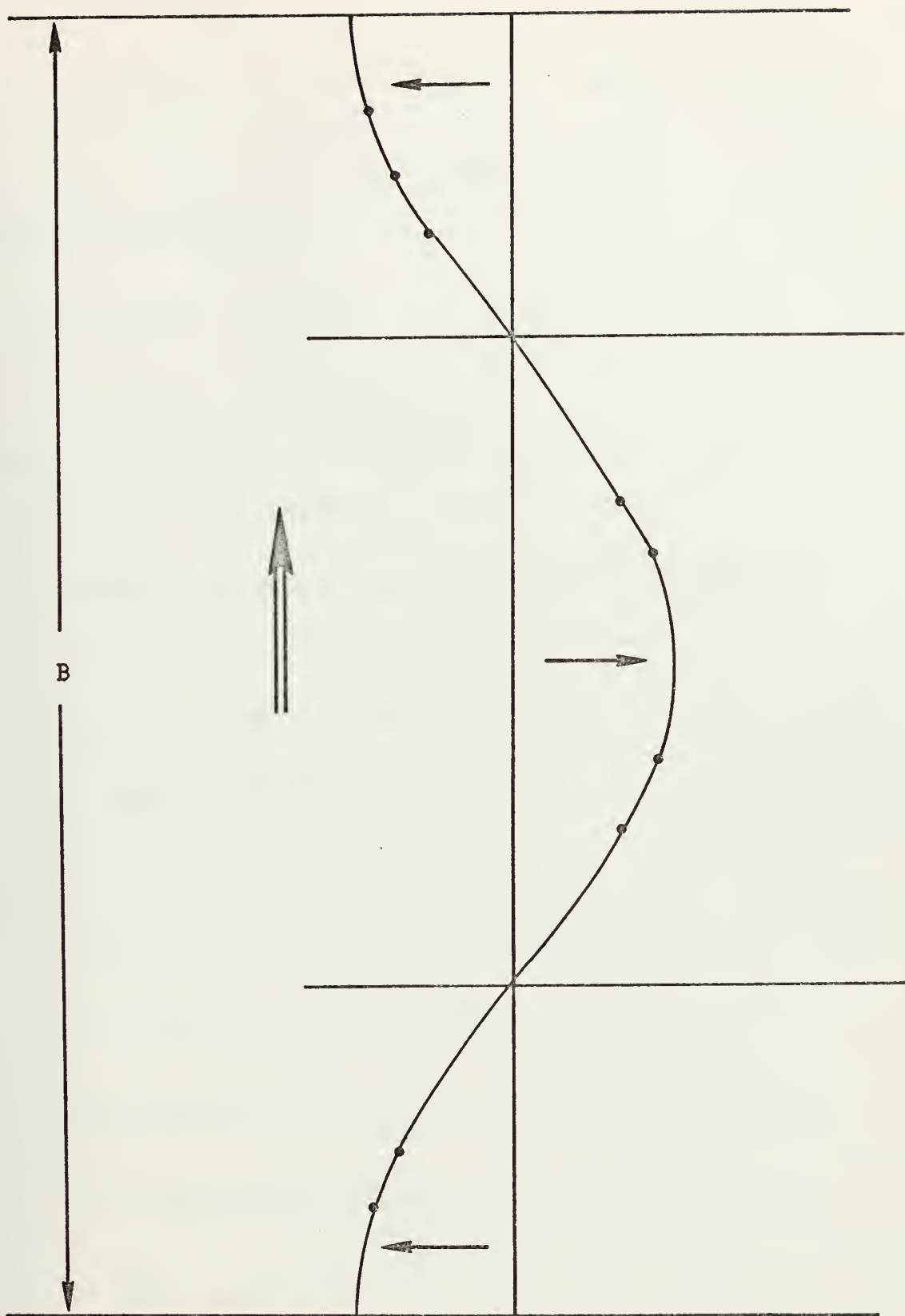


Figure 2: Wind Stress Pattern

$$u_{1,j} = -u_{2,j}$$

$$u_{34,j} = -u_{33,j}$$

$$v_{1,j} = -v_{2,j}$$

$$v_{34,j} = -v_{33,j},$$

(III-6)

and for the corners

$$(u,v)_{1,1} = (u,v)_{2,2} \quad (u,v)_{34,1} = (u,v)_{33,2}$$

$$(u,v)_{1,34} = (u,v)_{2,33} \quad (u,v)_{34,34} = (u,v)_{33,33} \quad (III-7)$$

where the original 32 x 32 (u,v) grid field becomes a 34 x 34 grid to include the boundary conditions.

B. FINITE DIFFERENCE FORM OF THE VORTICITY EQUATION

The finite difference form of (II-3) was written

$$\begin{aligned} \frac{\partial}{\partial t} \nabla^2 \psi_{i,j} + \beta \frac{(\psi_{i+1,j} - \psi_{i-1,j})}{2\Delta x} = \\ - \frac{1}{d} \left[\left(\frac{(V \cdot \nabla v)_{i+1,j+1} + (V \cdot \nabla v)_{i+1,j}}{2} \right) \right. \\ \left. - \left(\frac{(V \cdot \nabla v)_{i,j+1} + (V \cdot \nabla v)_{i,j}}{2} \right) \right] \\ + \frac{1}{d} \left[\left(\frac{(V \cdot \nabla u)_{i,j+1} + (V \cdot \nabla u)_{i+1,j+1}}{2} \right) \right. \\ \left. - \left(\frac{(V \cdot \nabla u)_{i,j} + (V \cdot \nabla u)_{i+1,j}}{2} \right) \right] \\ + \frac{1}{d} \left[\left(\frac{F_{yi+1,j+1} + F_{yi+1,j}}{2} \right) - \left(\frac{F_{yi,j+1} + F_{yi,j}}{2} \right) \right] \\ - \frac{1}{d} \left[\left(\frac{F_{xi,j+1} + F_{xi+1,j+1}}{2} \right) - \left(\frac{F_{xi,j} + F_{xi+1,j}}{2} \right) \right] \\ - \frac{2\pi F}{HB} \sin \left(\frac{2\pi}{B} y_j \right) d \end{aligned} \quad (III-8)$$

In (III-8) $\nabla^2 \psi_{i,j}$ is given by

$$\nabla^2 \psi_{i,j} = \frac{1}{d^2} [\psi_{i+1,j} + \psi_{i-1,j} + \psi_{i,j+1} + \psi_{i,j-1} - 4\psi_{i,j}].$$

The advection terms ($V \cdot \nabla u$, etc.) were finite differenced using the same method as Haney [1974], and the friction terms were expressed differently for each of the two forms of eddy viscosity as discussed below. Readers are referred to the documented computer program in Appendix A for further details.

In order to define F, it is first necessary to determine three values of minimum A (AMIN), such that the maximum in the analytic streamfunction (Ψ) is at $x = d/2, d, 2d$, respectively. Since the grid cannot resolve the western boundary in the first case (where the western boundary width is d), a large computational mode was expected with AMIN(1). The second case was expected to be marginally stable with AMIN(2); and finally, with AMIN(3) it was expected that the western boundary would be clearly resolved, but the value of AMIN(3) would be so high as to unrealistically damp the interior ocean solution. The respective difference equations for the three AMINs were:

$$\text{AMIN}(1) = \left(\beta \times \frac{\sqrt{3}}{2n} \times d/2 \right)^3$$

$$\text{AMIN}(2) = \left(\beta \times \frac{\sqrt{3}}{2n} \times d \right)^3$$

$$\text{AMIN}(3) = \left(\beta \times \frac{\sqrt{3}}{2n} \times 2d \right)^3 \quad (\text{III-9})$$

These three values of AMIN were used for the three fundamental experiments where A was taken as constant, and also for the minimum A in the experiments with non linear coefficients of eddy viscosity using (II-13) and (II-24) with $A_0 = \text{AMIN}$.

In determining the grid size and location for the non linear coefficients of eddy viscosity, the grid location of the generating parameters ($|\nabla\zeta|$ or $|D|$) had to be taken into consideration. This led to a 34×34 grid for $A(|\nabla\zeta|)$ in the case of enstrophy cascade, and a 33×33 grid for $A(|D|)$ in the kinetic energy cascade form. (See Figure 1).

1. Enstrophy Cascade Case

In the enstrophy cascade case, in order to generate coefficients of non linear eddy viscosity, it is necessary to generate a relative vorticity field and to determine the gradient of vorticity at each time step. Several possible techniques exist in developing a vorticity field, where in all cases vorticity would be defined on the 33×33 principal grid points (\cdot). For this model ζ was defined in terms of (u,v) by

$$\zeta = \frac{\partial v}{\partial x} - \frac{\partial u}{\partial y} =$$

$$\zeta_{i,j} = \frac{VAV_{i+1,j} - VAV_{i,j}}{d} - \frac{UAV_{i,j+1} - UAV_{i,j}}{d} \quad (III-10)$$

$$i = 1 \dots 33, j = 1 \dots 33$$

where UAV and VAV are defined as

$$UAV_{i,j} = \frac{U_{i,j} + U_{i+1,j}}{2} ; \quad VAV_{i,j} = \frac{V_{i,j} + V_{i,j+1}}{2} , \quad (III-11)$$

$$i = 1 \dots 33, j = 1 \dots 34; i = 1 \dots 34, j = 1, 33$$

in order to get an equivalent (u,v) on the principal grid points. If (u,v) are written in terms of Ψ , then (III-10) reduces to

$$\zeta_{i,j} = \frac{1}{2d^2} (\Psi_{i+1,j+1} + \Psi_{i+1,j-1} + \Psi_{i-1,j-1} + \Psi_{i-1,j+1} - 4\Psi_{i,j}) \quad (III-12)$$

24

This method, along with three other schemes of Miyakoda [1962] for calculating vorticity, were utilized and compared.

The gradient of vorticity ($|\nabla\zeta|$) was developed using centered differences on the 32 x 32 grid centers ($^{\circ}$):

$$|\nabla\zeta|_{i,j} = \left\{ \left[\frac{1}{d} \left(\frac{\zeta_{i,j} + \zeta_{i,j-1}}{2} - \frac{\zeta_{i-1,j} + \zeta_{i-1,j-1}}{2} \right) \right]^2 + \left[\frac{1}{d} \left(\frac{\zeta_{i,j} + \zeta_{i-1,j}}{2} - \frac{\zeta_{i,j} + \zeta_{i-1,j-1}}{2} \right) \right]^2 \right\}^{1/2}$$

$$i = 2 \dots 33, j = 2 \dots 33 \quad (\text{III-13})$$

Finally, (II-13) in finite difference form

$$A(|\nabla\zeta|)_{i,j} = \text{AMIN} \times (1 + m \times \frac{|\nabla\zeta|_{i,j}}{|\nabla\zeta|_{\max}})$$

$$i = 2 \dots 33, j = 2 \dots 33 \quad (\text{III-14})$$

where $A_{i,j}$ is defined on the 32 x 32 grid centers. The value of $|\nabla\zeta|_{\max}$ of 6×10^{14} was estimated from linear theory [Munk, 1950], and m was considered an adjustable parameter.

The finite difference form of the friction force for enstrophy cascade, on a 32 x 32 grid, was written from (II-14) and (II-15) as

$$F_{x_{i,j}} = \frac{1}{d^2} \left[\left(\frac{A_{i,j} + A_{i+1,j}}{2} \right) (U_{i+1,j} - U_{i,j}) - \left(\frac{A_{i-1,j} + A_{i,j}}{2} \right) (U_{i,j} - U_{i-1,j}) \right]$$

$$+ \frac{1}{d^2} \left[\left(\frac{A_{i,j} + A_{i,j+1}}{2} \right) (U_{i,j+1} - U_{i,j}) - \left(\frac{A_{i,j-1} + A_{i,j}}{2} \right) (U_{i,j} - U_{i,j-1}) \right]$$

$$i = 2 \dots 33, j = 2 \dots 33$$

$$\begin{aligned}
Fy_{i,j} = & \frac{1}{d^2} \left[\left(\frac{A_{i,j} + A_{i+1,j}}{2} \right) (v_{i+1,j} - v_{i,j}) \right. \\
& - \left. \left(\frac{A_{i-1,j} + A_{i,j}}{2} \right) (v_{i,j} - v_{i-1,j}) \right] \\
& + \frac{1}{d^2} \left[\left(\frac{A_{i,j} + A_{i,j+1}}{2} \right) (v_{i,j+1} - v_{i,j}) \right. \\
& - \left. \left(\frac{A_{i,j-1} + A_{i,j}}{2} \right) (v_{i,j} - v_{i,j-1}) \right] \quad (III-15)
\end{aligned}$$

$i = 2 \dots 33, j = 2 \dots 33$

It is clear that (III-15) requires a 34 x 34 field of $A(|\nabla\zeta|)$ in order to calculate the friction forces. Two methods were utilized to generate a value of $|\nabla\zeta|$ and thereby a value of eddy viscosity coefficients across the boundary. The first case was linear extrapolation in all four directions. For the western boundary the finite difference form of $A(|\nabla\zeta|)$ was

$$\begin{aligned}
\text{SLOPE} &= (A_{2,j} - A_{3,j})/d \\
A_{1,j} &= \text{SLOPE} \times d + A_{2,j} \quad (III-16) \\
j &= 2, \dots, 33
\end{aligned}$$

and the values of A immediately outside the other boundaries were determined in a similar manner. This method is physically representative because it gives a boundary of increasing coefficients in the direction of the western boundary. Along the other boundaries the gradient, and hence the boundary value of $A(|\nabla\zeta|)$ is flat.

The second method utilized to generate a value for $A(|\nabla\zeta|)$ across the boundary was to extend the existing interior "boundary" outwards in all four directions, so that across the western boundary, for example

$$A_{1,j} = A_{2,j} \quad j = 2, \dots, 33 \quad (\text{III-17})$$

This method is consistent with the antisymmetric velocity profile which accompanies the zero flow boundary conditions. In both cases the 34 x 34 corners were not used for $A(|\nabla \zeta|)$.

The curl of the friction force, defined on a 31 x 31 interior grid, was

$$\begin{aligned} \text{CURL } F_{i,j} = & \left(\frac{F_{yi,j} + F_{yi,j-1}}{2} - \frac{F_{yi-1,j} + F_{yi-1,j-1}}{2} \right) / d \\ & - \left(\frac{F_{xi-1,j} + F_{xi,j}}{2} - \frac{F_{xi-1,j-1} + F_{xi,j-1}}{2} \right) / d \\ & i = 3 \dots 33 \quad j = 3 \dots 33 \quad (\text{III-18}) \end{aligned}$$

2. Kinetic Energy Cascade Case

The first steps in determining the deformation field of the fluid was 1) to calculate the shearing deformation (D_s)

$$\begin{aligned} D_{si,j} = & \frac{VAV_{i+1,j} - VAV_{i,j}}{d} + \frac{UAV_{i,j+1} - UAV_{i,j}}{d} \quad (\text{III-19}) \\ & i = 1..33 \quad j = 1 \dots 33 \end{aligned}$$

where UAV and VAV are defined in (III-11), and 2) to calculate the stretching deformation (D_t)

$$\begin{aligned} D_{ti,j} = & \frac{UAVE_{i+1,j} - UAVE_{i,j}}{d} - \frac{VAVE_{i,j+1} - VAVE_{i,j}}{d} \quad (\text{III-20}) \\ & i = 1..33 \quad j = 1 \dots 33 \end{aligned}$$

where UAVE and VAVE are defined as

$$\begin{aligned} UAVE_{i,j} = & \frac{U_{i,j} + U_{i,j+1}}{2} & i = 1, \dots, 34 \\ & j = 1, \dots, 33 \\ VAVE_{i,j} = & \frac{V_{i,j} + V_{i+1,j}}{2} & i = 1 \dots 33 \\ & j = 1 \dots 34 \quad (\text{III-21}) \end{aligned}$$

Then the square root of the squares of the values of

deformation along and normal to a streamline gave the value of deformation at each principal grid point (•):

$$|D|_{i,j} = [(D_{si,j})^2 + (D_{ti,j})^2]^{1/2} \quad (\text{III-22})$$

$$i = 1 \dots 33 \quad j = 1 \dots 33$$

Next, equation (II-25) in finite difference form was used to calculate values for $A(|D|)$ based on kinetic energy cascade

$$A(|D|)_{i,j} = \text{AMIN}(1 - m \times \frac{|D_{i,j}|}{|D_{\max}|}) \quad (\text{III-23})$$

$$i = 1 \dots 33 \quad j = 1 \dots 33$$

where AMIN and m are as described above, and the maximum deformation (D_{\max}) was estimated to be 6.22×10^{-7} . Since $A(|D|)$ was a 33×33 field, the form of the friction force did not require additional boundary conditions for $A(|D|)$.

The numerical form for the friction forces based on $A(|D|)$ written from (II-14) and (II-15) was

$$\begin{aligned} F_{xi,j} = & \frac{1}{d^2} [(\frac{A_{i,j-1} + A_{i,j}}{2})(u_{i+1,j} - u_{i,j}) \\ & - (\frac{A_{i-1,j-1} + A_{i-1,j}}{2})(u_{i,j} - u_{i-1,j})] \\ & + \frac{1}{d^2} [(\frac{A_{i,j} + A_{i-1,j}}{2})(u_{i,j+1} - u_{i,j}) \\ & - (\frac{A_{i,j} + A_{i-1,j-1}}{2})(u_{i,j} - u_{i,j-1})] \end{aligned}$$

$$\begin{aligned} F_{yi,j} = & \frac{1}{d^2} [(\frac{A_{i,j-1} + A_{i,j}}{2})(v_{i+1,j} - v_{i,j}) \\ & - (\frac{A_{i-1,j-1} + A_{i-1,j}}{2})(v_{i,j} - v_{i-1,j})] \\ & + \frac{1}{d^2} [(\frac{A_{i,j} + A_{i-1,j}}{2})(v_{i,j+1} - v_{i,j}) \end{aligned}$$

$$- \frac{(A_{i,j-1} + A_{i-1,j-1})}{2} (v_{i,j} - v_{i,j-1}) \quad (\text{III-24})$$

The Smagorinsky form of the friction force for $A \sim |D|$ from (II-26) and (II-27) was

$$\begin{aligned} F_{xi,j} = & \frac{1}{d} \{ [(A_{i,j} + A_{i,j-1})/2] [(D_{ti,j} + D_{ti,j-1})/2] \\ & - [(A_{i-1,j} + A_{i-1,j-1})/2] [(D_{ti-1,j} + D_{ti-1,j-1})/2] \\ & + [(A_{i,j} + A_{i-1,j})/2] [(D_{si,j} + D_{si-1,j})/2] \\ & - [(A_{i,j-1} + A_{i-1,j-1})/2] [(D_{si-1,j-1})/2] \} \\ F_{yi,j} = & \frac{1}{d} \{ [(A_{i,j} + A_{i,j-1})/2] [(D_{si,j} + D_{si,j-1})/2] \\ & - [(A_{i-1,j} + A_{i-1,j-1})/2] [(D_{si-1,j-1})/2] \\ & + [(A_{i,j} + A_{i-1,j})/2] [(D_{ti,j} + D_{ti-1,j})/2] \\ & - [(A_{i,j-1} + A_{i-1,j-1})/2] [(D_{ti,j-1} + D_{ti-1,j-1})/2] \} \\ & i = 2 \dots 33, \quad j = 2 \dots 33 \quad (\text{III-25}) \end{aligned}$$

The finite difference form of the curl of the friction force is the same as for the enstrophy cascade case (III-18).

3. Solution Description

Using (III-8) as the basis for solution, a centered time difference scheme (Leapfrog) was used for all terms except the friction terms which were evaluated at the previous time step. With time steps of fourteen hours, equation (III-8) was integrated for 210 days. To start the model and to prevent solution separation, the Euler-Backward (Matsuno) time scheme was utilized for the first and every fifty time steps. In the

kinetic energy cascade experiments the form of the friction force shown in the following results was in accordance with equation (III-24). Experiments were also conducted using the Smagorinsky form (III-25) which gave similar results to (III-24) and therefore are not shown in this study.

The solution phase of the model had to solve the equation

$$\nabla^2 \left(\frac{\partial \Psi}{\partial t} \right) - F_1 = 0 \quad (\text{III-26})$$

for the tendency $\partial \Psi / \partial t$. This was done using a direct Poisson solver. This new technique was written by R. Sweet [1972], based on a method originated by Buneman [1969], and revised for this model by Professor F. Faulkner of the Naval Postgraduate School. The method is extremely accurate and made possible computer time savings of nearly an order of magnitude.

IV. RESULTS

A. RESTATEMENT OF PURPOSE

The main purpose of this thesis was to present a scheme whereby the accuracy of the numerical solution of a finite grid ocean circulation model would be improved by the introduction of non linear lateral eddy viscosity coefficients. As shown in earlier chapters, the gradient of relative vorticity or the fluid deformation could be used as the respective parameters to generate the coefficients of eddy viscosity. The solutions using constant coefficients of lateral eddy viscosity will be compared with those using variable coefficients derived from enstrophy cascade ($A \sim |\nabla \zeta|$) and kinetic energy cascade ($A \sim |D|$) respectively.

B. ANALYTICAL CONSIDERATIONS

The initial experiments investigated three cases of constant coefficients of eddy viscosity. First, an accurate analytical solution for the streamfunction was made by means of a separate model where grid spacing was 60 km. The analytical solution of the streamfunction in terms of the wind stress curl was developed by Munk [1950], who considered a linear eddy viscosity:

$$\psi(x,y) = -rX(x)\beta^{-1}\text{CURL}_z\tau \quad (\text{IV-1})$$

where r = domain width, $\text{curl}_z\tau$ = the k component of the wind stress curl, and

$$X(x) = Ke^{-1/2 kx} \cos\left(\frac{\sqrt{3}}{2} kx + \frac{\sqrt{3}}{2kr} - \frac{\pi}{6}\right) + 1 \\ - \frac{1}{kr} (kx - e^{-k(r-x)} - 1)$$

in which $X(x)$ = distance eastward from the western boundary,

$$k = (\beta/A)^{1/3} \quad \text{and} \quad K = \frac{2}{\sqrt{3}} - \frac{\sqrt{3}}{kr}$$

The reader is referred to Figure 3 which portrays the analytical streamfunction (ψ) for the three cases where the maximum of ψ occurs at $d/2$, d and $2d$, respectively. The three values of A which permitted the above analytical situation to occur were the three constant coefficients of eddy viscosity now examined in the numerical model.

C. EXPERIMENTS WITH CONSTANT COEFFICIENTS OF EDDY VISCOSITY

The first constant coefficient of eddy viscosity, $A_1 = 0.12 \times 10^8 \text{ cm}^2 \text{ sec}^{-1}$, which physically represents the interior ocean circulation most accurately, produces a large amplitude computational oscillation which fills the entire basin of the numerical model. Figure 4 shows the extent of the oscillation produced in the ψ field by this relatively low magnitude coefficient of eddy viscosity. Figure 7 shows a direct comparison of the analytical ψ field and the numerical ψ field produced by A_1 at the latitude of maximum wind stress curl. The reader is also referred to Table I which presents a tabular comparison of ψ field highlights as generated by constant eddy viscosity coefficients. All of these features are in accordance with the study by Takano [1975].

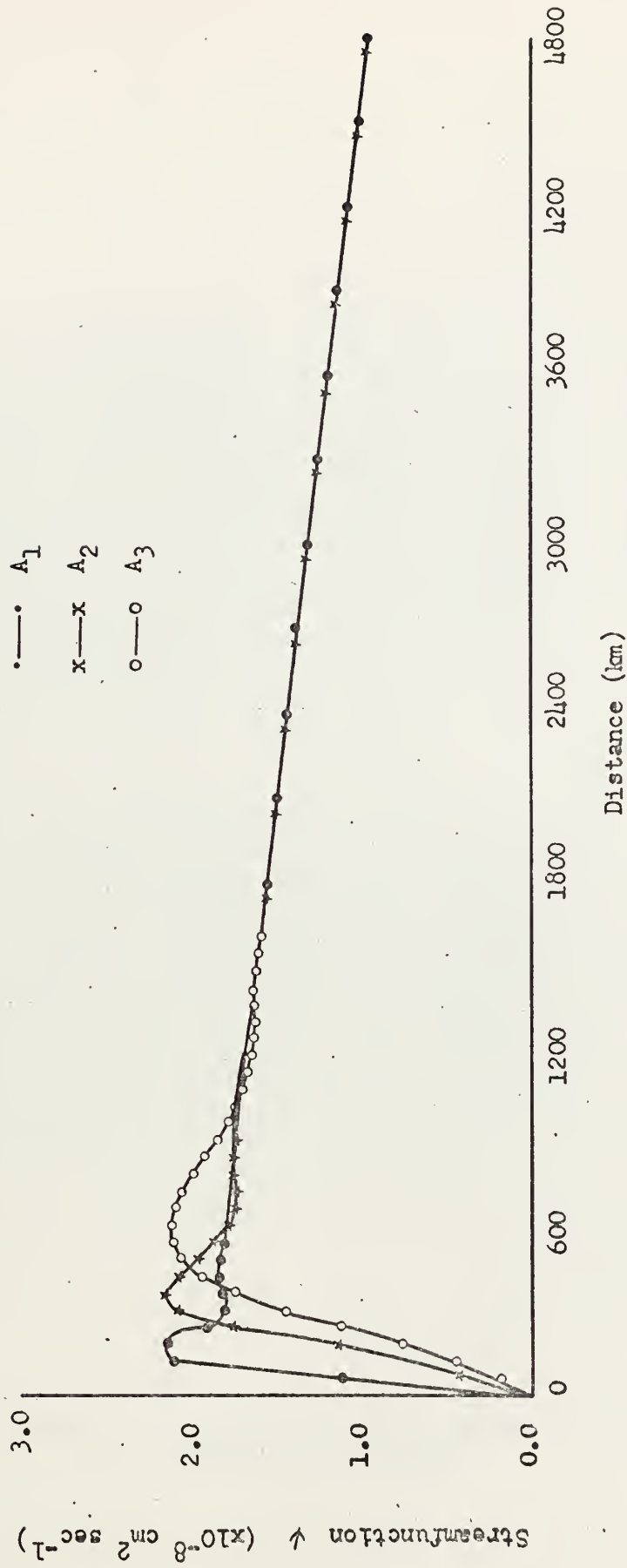


Figure 3: Analytical Solutions of ψ at Latitude with Maximum Streamfunction for A_1 , A_2 , and $A_3 = \text{Constants}$

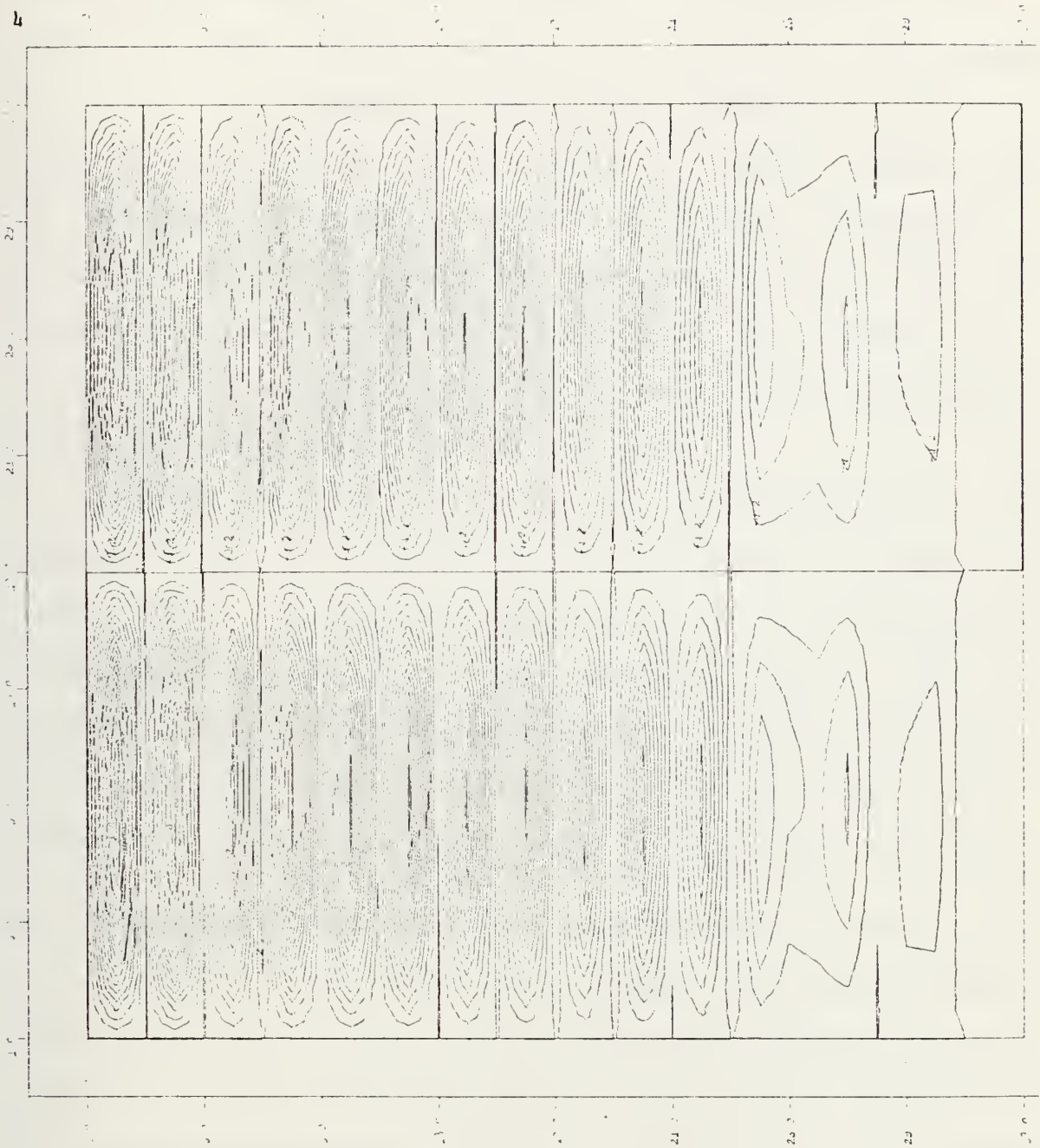


Figure 4: Numerical Solution of Streamfunction
for $A_1 = \text{Constant}$

Next, $A_2 = 0.93 \times 10^8 \text{ cm}^2 \text{ sec}^{-1}$, an order of magnitude larger coefficient of eddy viscosity, was examined in the numerical model. Figure 5 shows the circulation for constant A_2 ; Figure 11, a graphical comparison of analytical and numerical ψ field for A_2 ; and Table I, a tabular comparison. A_2 , used as a constant, produced a marginally satisfactory solution, where the western boundary current was rather well represented, but a moderate computational oscillation was still evident with the value of the maximum streamfunction 50% higher than the analytical solution.

By increasing the coefficient yet another order of magnitude to $A_3 = 7.5 \times 10^8 \text{ cm}^2 \text{ sec}^{-1}$ (Figure 6, Figure 14, and Table I), the computational oscillation is negligible with only about 3% error in the numerical solution. The western boundary current placement was in accord with the analytical case (Figure 3), but the solution in the ocean interior was unrealistically damped by the large viscosity.

D. EXPERIMENTS WITH NON LINEAR COEFFICIENTS OF EDDY VISCOSITY

It is clear that there is no single coefficient of eddy viscosity that can physically or numerically depict all the aspects of fluid circulation both in the ocean interior and in the western boundary. As can be observed from the results so far, the objective of using non linear eddy viscosity is to have low coefficients of eddy viscosity in the ocean interior, and increasing coefficients approaching the western boundary in order to resolve the western boundary current and to prevent the development of a computational mode in the solution.

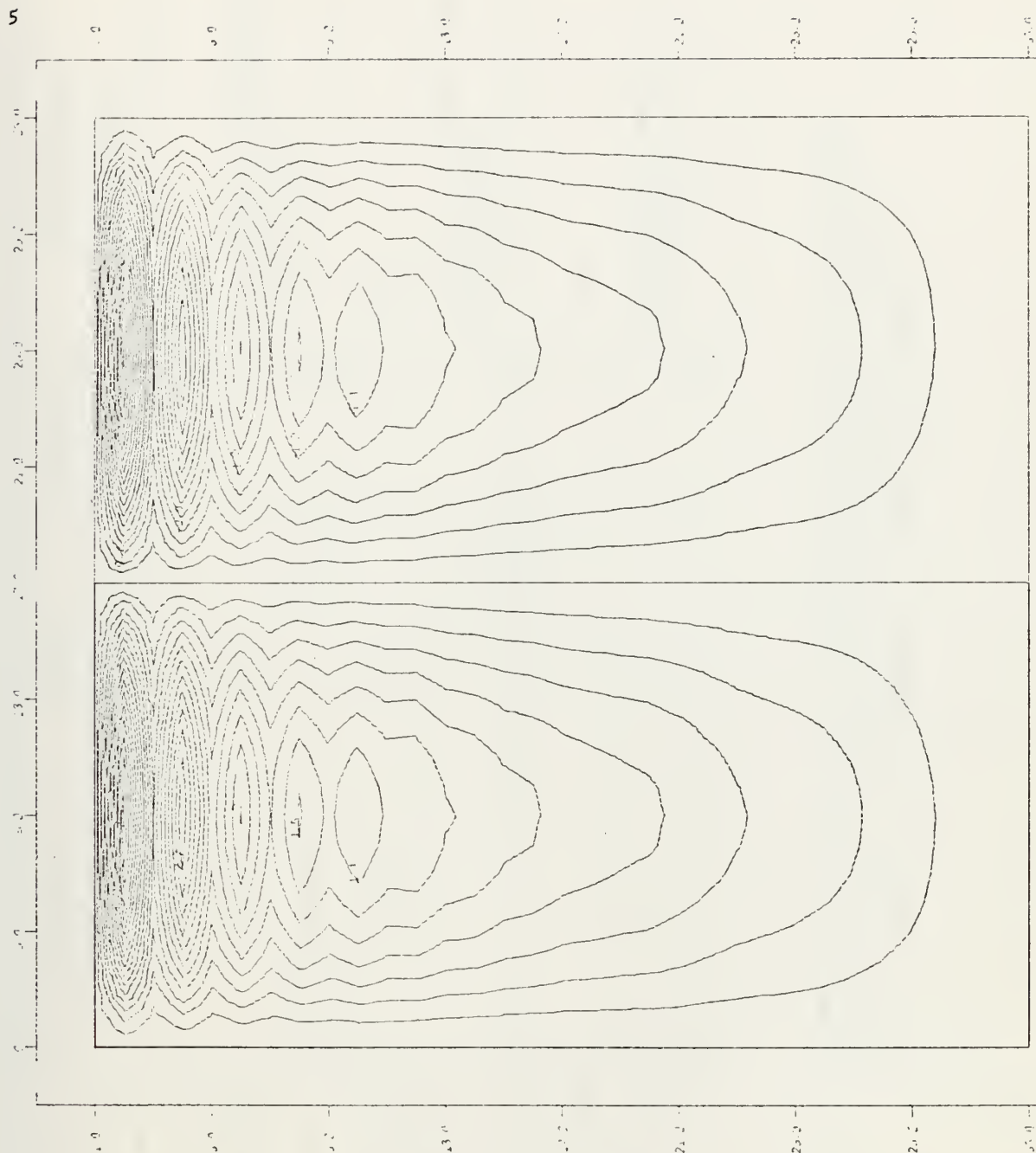


Figure 5: Numerical Solution of Streamfunction
for $A_2 = \text{Constant}$

Figure Number	Type of Solution	A = constant = ($\times 10^8 \text{ cm}^2 \text{ sec}^{-1}$)	ψ_{max} ($\times 10^8 \text{ cm}^2 \text{ sec}^{-1}$)	Location of ψ_{max}	Description of Solution
4	Analytical	.12	2.19	d/2	None
	Numerical	.12	3.72	d	Very heavy computational oscillations
5	Analytical	.93	2.17	d	None
	Numerical	.93	3.26	d	Moderate computational oscillations
6	Analytical	7.5	2.13	2d	None
	Numerical	7.5	2.07	2d	Negligible computational oscillation

TABLE I: Summary of results for significant numerical experiments with constant coefficients of lateral eddy viscosity A_1 , A_2 , and A_3 as compared to analytical results.

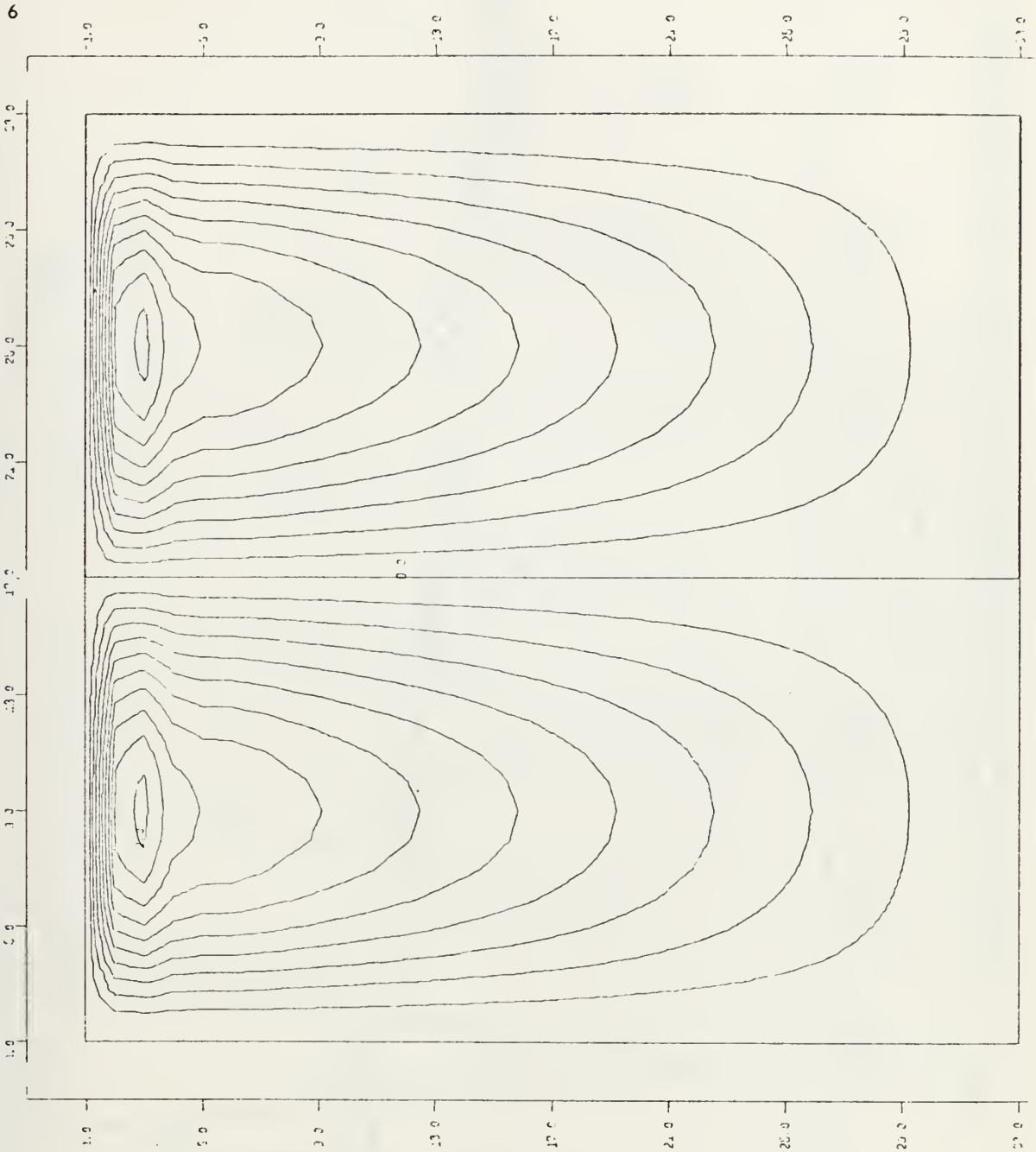


Figure 6: Numerical Solution of Streamfunction
for $\Lambda_3 = \text{Constant}$

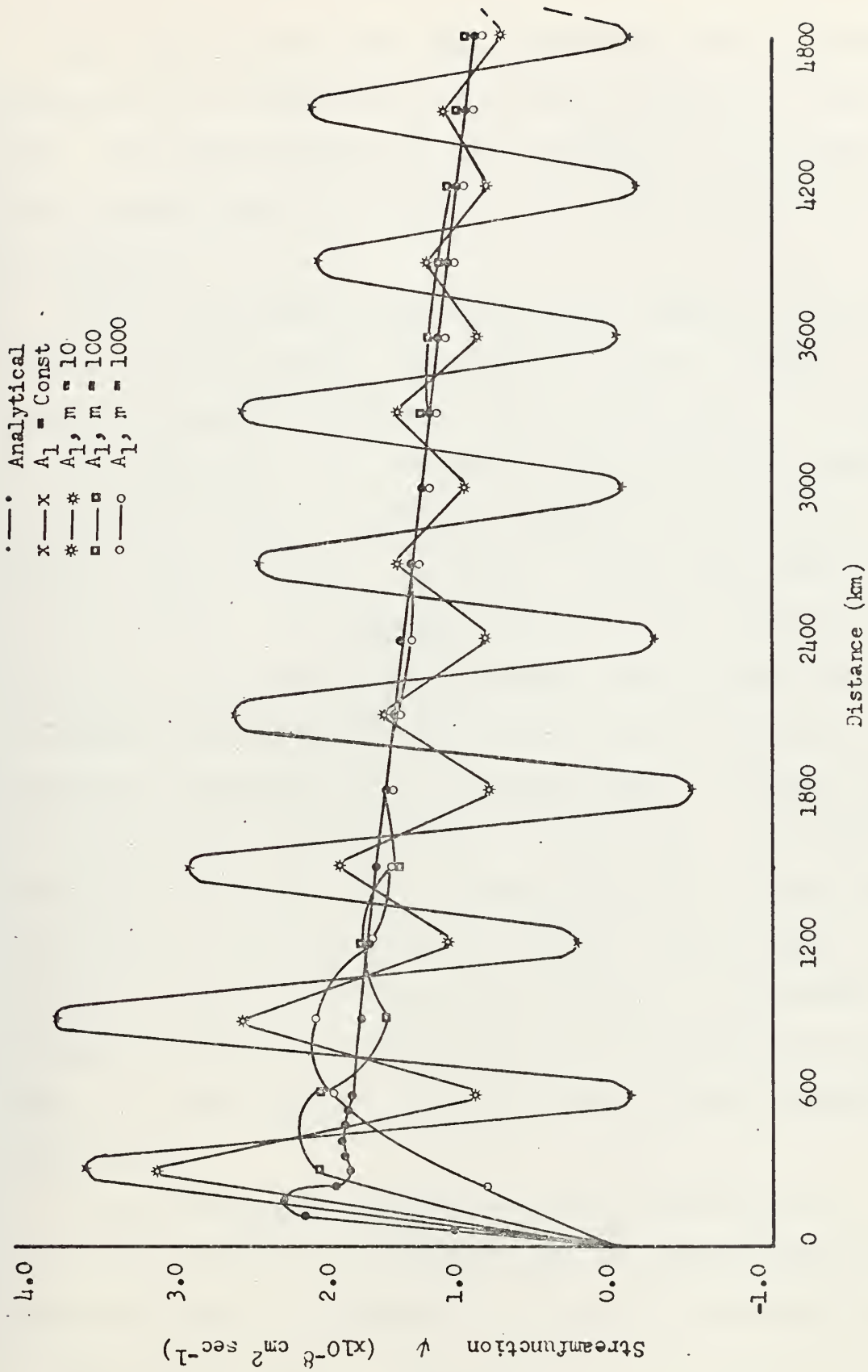


Figure 7: Numerical and Analytical Solutions of ψ at Latitude with Maximum Streamfunction for Non Linear Experiments with A_1 , Kinetic Energy Cascade Case

Non linear coefficients that represent actual physical processes in the ocean were developed in Chapters II and III. It is shown below that if the limits of the range of these coefficients are properly chosen the desired objective is achieved.

In the first non linear experiments, ranges of coefficients of eddy viscosity were chosen with the minimum coefficient equal to $AMIN(1) = A_1$, and the range of variation of the coefficients was governed by the adjustable parameter m in both (II-13) for enstrophy cascade and (II-25) for kinetic energy cascade. Of course, in this case where $AMIN$ is the smallest, the greatest range of m was required to properly resolve the western boundary and to prevent an unacceptable computational oscillation from developing in the solution. Experiments were conducted with m varying from 10 to 1000 with results that are noted below. It should be noted that the value for m is not precisely a direct multiplier for the range of A due to the non linear effect of $|\nabla\zeta_{max}|$ in (III-14) and $|D|_{max}$ in (III-15). The actual values of $A/AMIN$ were printed out in the experiments and the range of $A/AMIN$ appears in Table II for the most significant experiments.

In the enstrophy cascade ($A \sim |\nabla\zeta|$) experiment for $A_1 = 0.12 \times 10^8$ and $m = 10$ and using the symmetrical boundary conditions for A as indicated in (III-17), the actual range of A/A_1 was 1.0 to 7.0. The resulting ψ field can be seen in Figure 8A. Using the linear extrapolation shown in

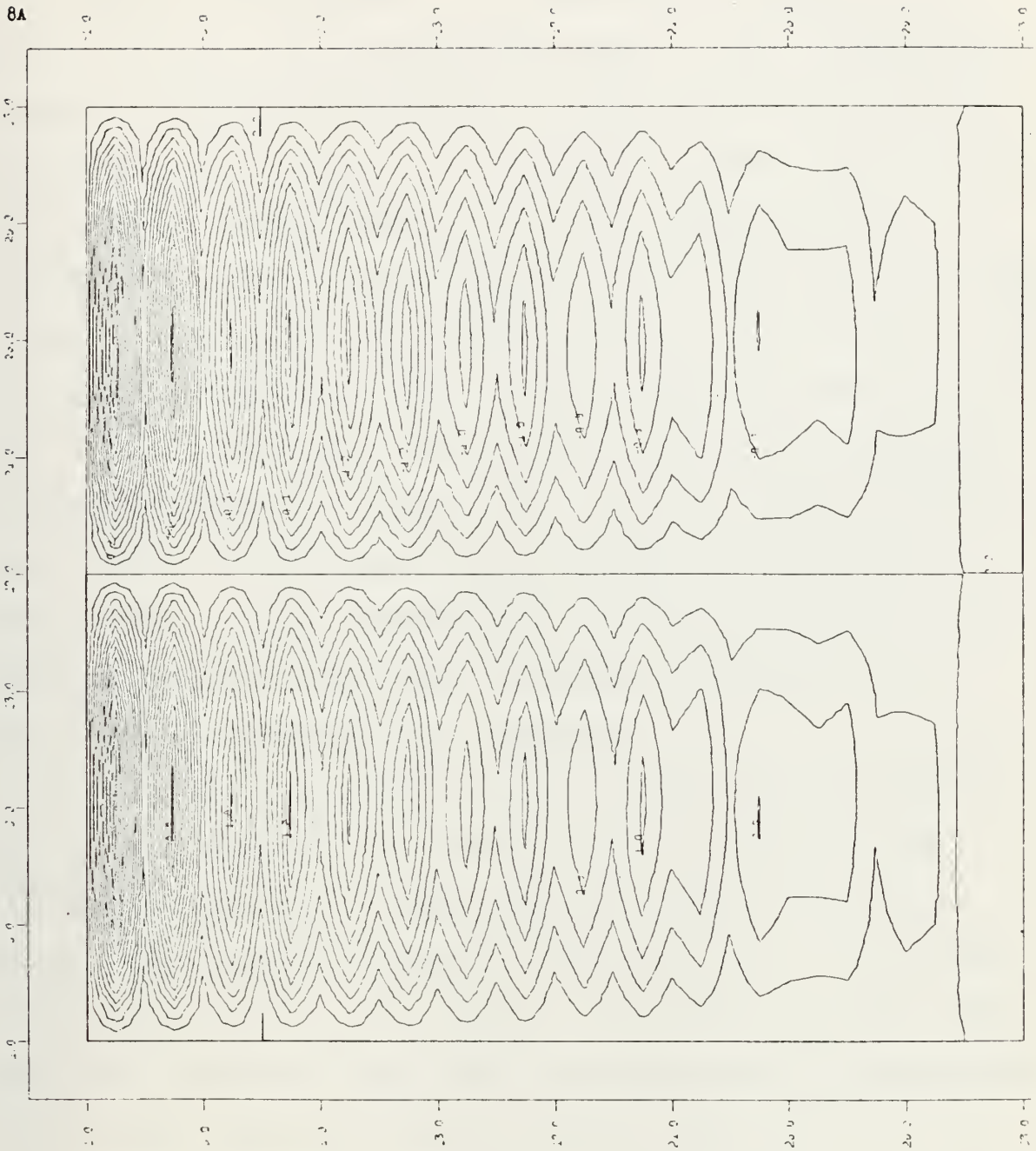


Figure 8A: Numerical Solutions of Ψ for A_1 and $m = 10$
Symmetric Boundary Conditions for $A \sim |\nabla \zeta|$

(III-16) to obtain A across the boundary, the solution shown in Figure 8B was obtained. In this case the range of A/A_1 was 1.2 to 7.9. It is noted here that in the extrapolation boundary condition the maximum A occurs outside the western boundary and therefore is artificially derived; and that the A/A_1 minimum values indicated in these experiments are not actually the lowest ratio obtained, but a value representative of the A obtained in the interior ocean. In the kinetic energy cascade experiment ($A \sim |D|$) for this case, the range of A/A_1 was 1.1 to 10.8, with results very similar to the enstrophy cascade experiments (Figure 8C). As can be readily seen in the figures for the above three experiments with $A_{\min} = A_1$ and $m = 10$, a heavy computational oscillation is still very much in existence, although a definite improvement over $A_1 = \text{constant}$ (Figure 4) is apparent.

It can also be noted here and in the following experiments, that although the method used in deriving the non linear coefficients of eddy viscosity, namely $A \sim |\nabla \zeta|$ and $A \sim |D|$, show somewhat different characteristics in the ocean circulation pattern, the results were analogous enough that the main purpose of this thesis could have been accomplished with either method and either boundary conditions for A in the case of $A \sim |\nabla \zeta|$. In addition, several tests using various combinations of the Laplacian given by (III-12) and the usual 5-point Laplacian were made. It was found that the method of defining the relative vorticity field was of no consequence in the results achieved, and therefore this paper does not

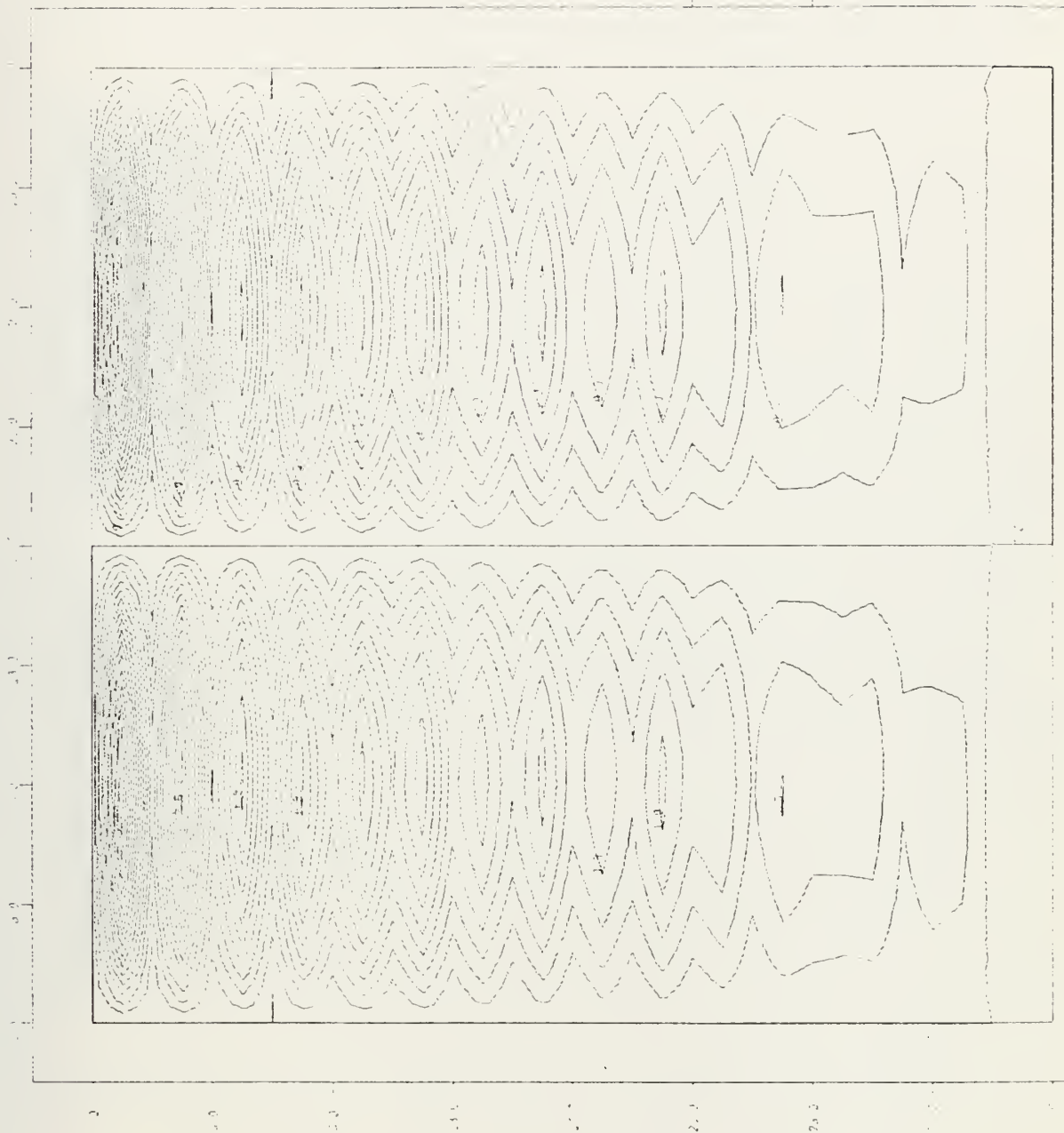


Figure 8B: Numerical Solutions of Ψ for Λ_1 and $m = 10$
 Extrapolated Boundary Conditions for $\Lambda \sim |\nabla \zeta|$

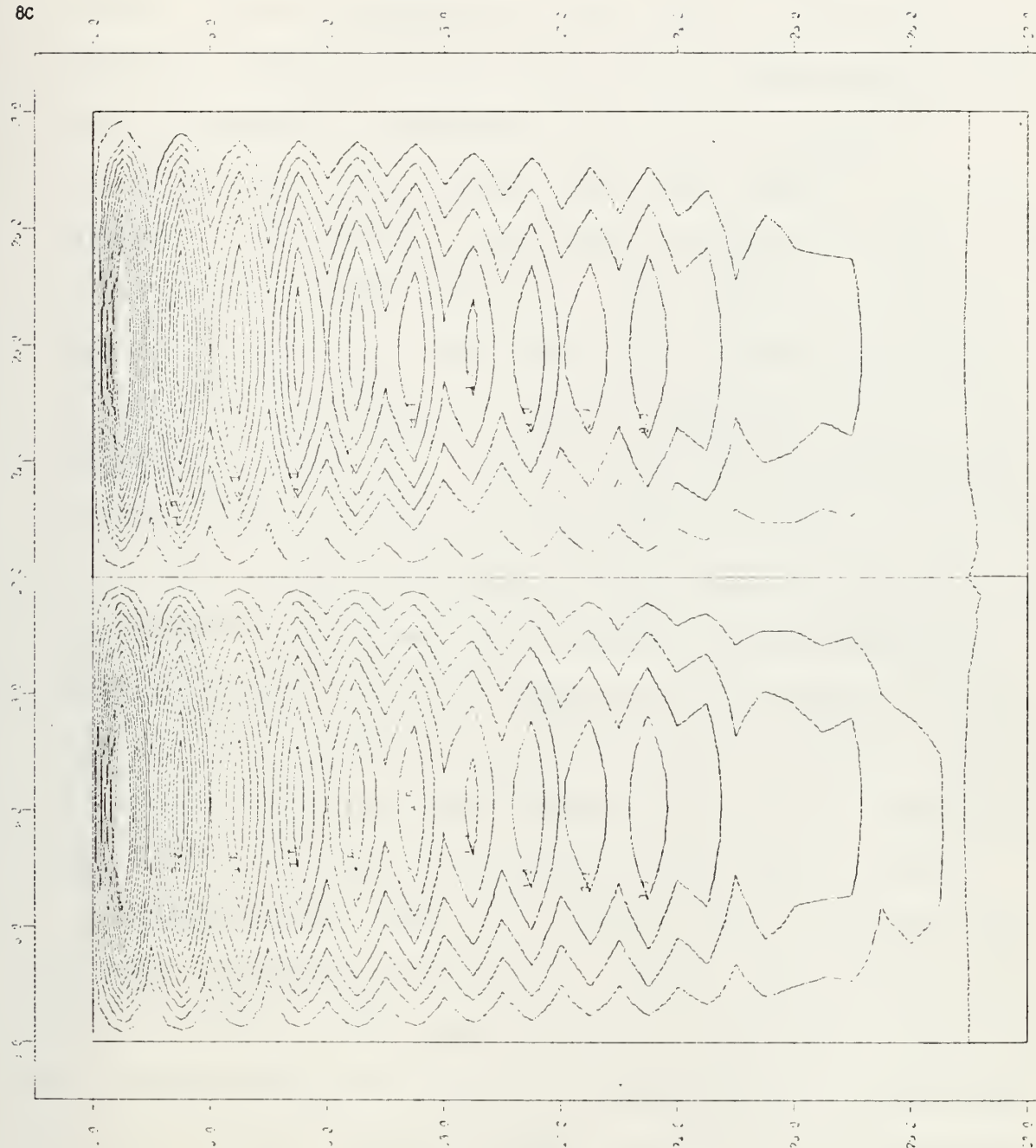


Figure 8C: Numerical Solutions of Ψ for A_1 and $m = 10$, $A \sim |D|$

warrant any further discussion of this aspect. In all the above non linear experiments with A_1 , in addition to the figures listed and Table II, the reader is referred to the graphical representation of the steady state maximum analytical and numerical streamfunction field in Figure 7.

In the next set of experiments with AMIN(1), m is increased to 100 giving a two order of magnitude range for the coefficients of eddy viscosity. The results are shown in Figures 9A, 9B, 9C, 7, and Table II. In the cases where $A \propto |\nabla \zeta|$ with the symmetric boundary conditions for A , A/A_1 ranged from 1.2 to 41.7, and for the linear extrapolation boundary conditions A/A_1 ranged from 1.3 to 62.2. For $A \propto |D|$ the values of the coefficients ranged from 1.5 to 70.1. In this group of experiments the solution of streamfunction improved greatly, with the numerical ψ_{\max} within a few per cent of the analytical ψ_{\max} in all cases. However, the higher value of A at the western boundary resulted in a tendency for ψ_{\max} to move eastward, especially in the case of $A \propto |D|$.

Increasing the range of A_1 another order of magnitude, the next experiments examined $m = 1000$. These results are shown in Figures 10A, 10B, 10C, 7, and Table II. In all cases the computational oscillation was negligible, the interior solution was not strongly damped, and the western boundary region was well defined. The variation of A/A_1 was 1.5 to 165 for $A \propto |\nabla \zeta|$ (symmetric boundary conditions), 1.6 to 237 for $A \propto |\nabla \zeta|$ (extrapolated boundary condition), and 5.0 to 313 for $A \propto |D|$. Again, however, there was a tendency for ψ_{\max} to

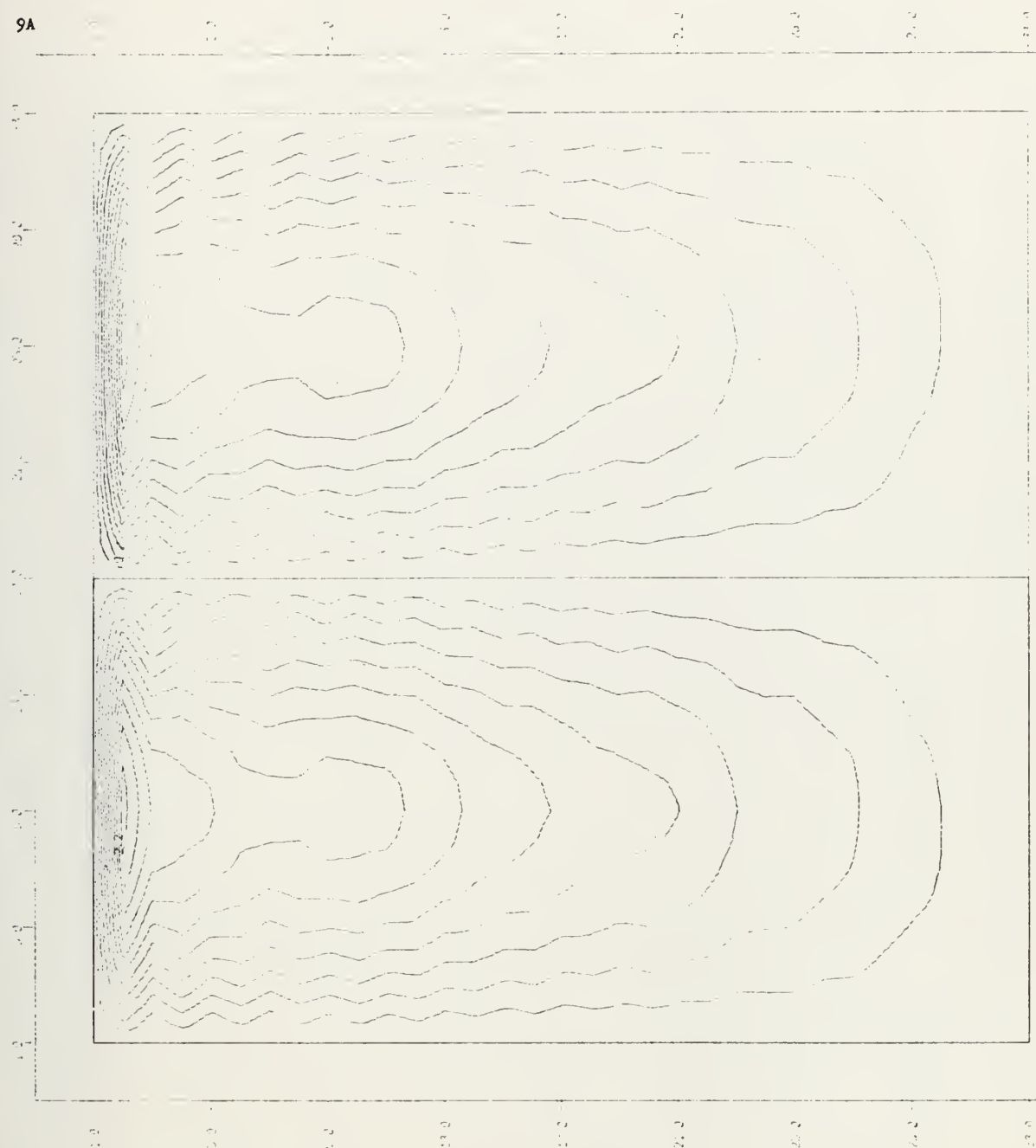


Figure 9A: Numerical Solutions of Ψ for Λ_1 and $m = 100$
Symmetric Boundary Conditions for $\Lambda \sim |V_\zeta|$

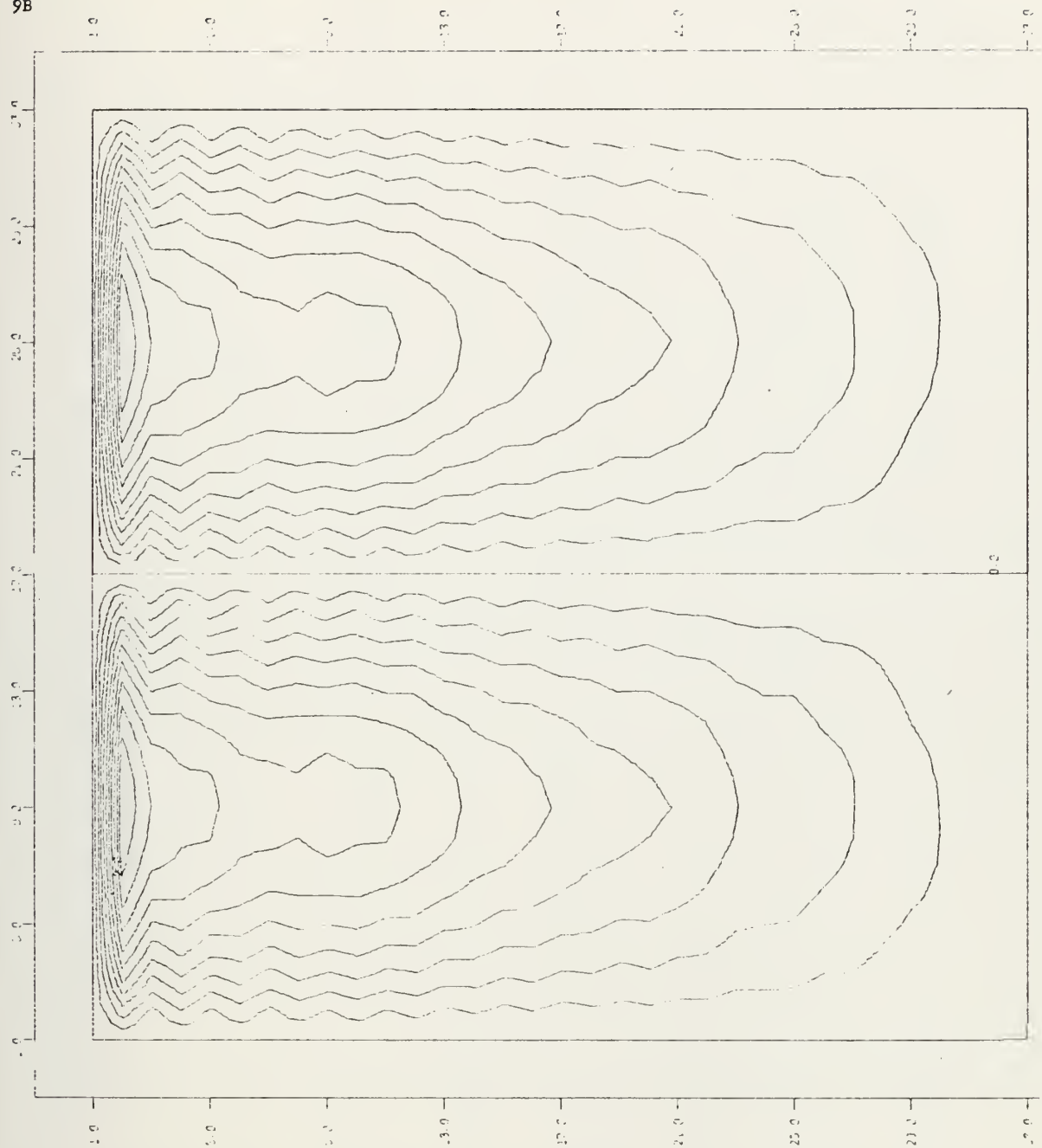


Figure 9B: Numerical Solutions of ψ for Λ_1 and $m = 100$
 Extrapolated Boundary Conditions for $\Lambda \sim |\nabla \zeta|$

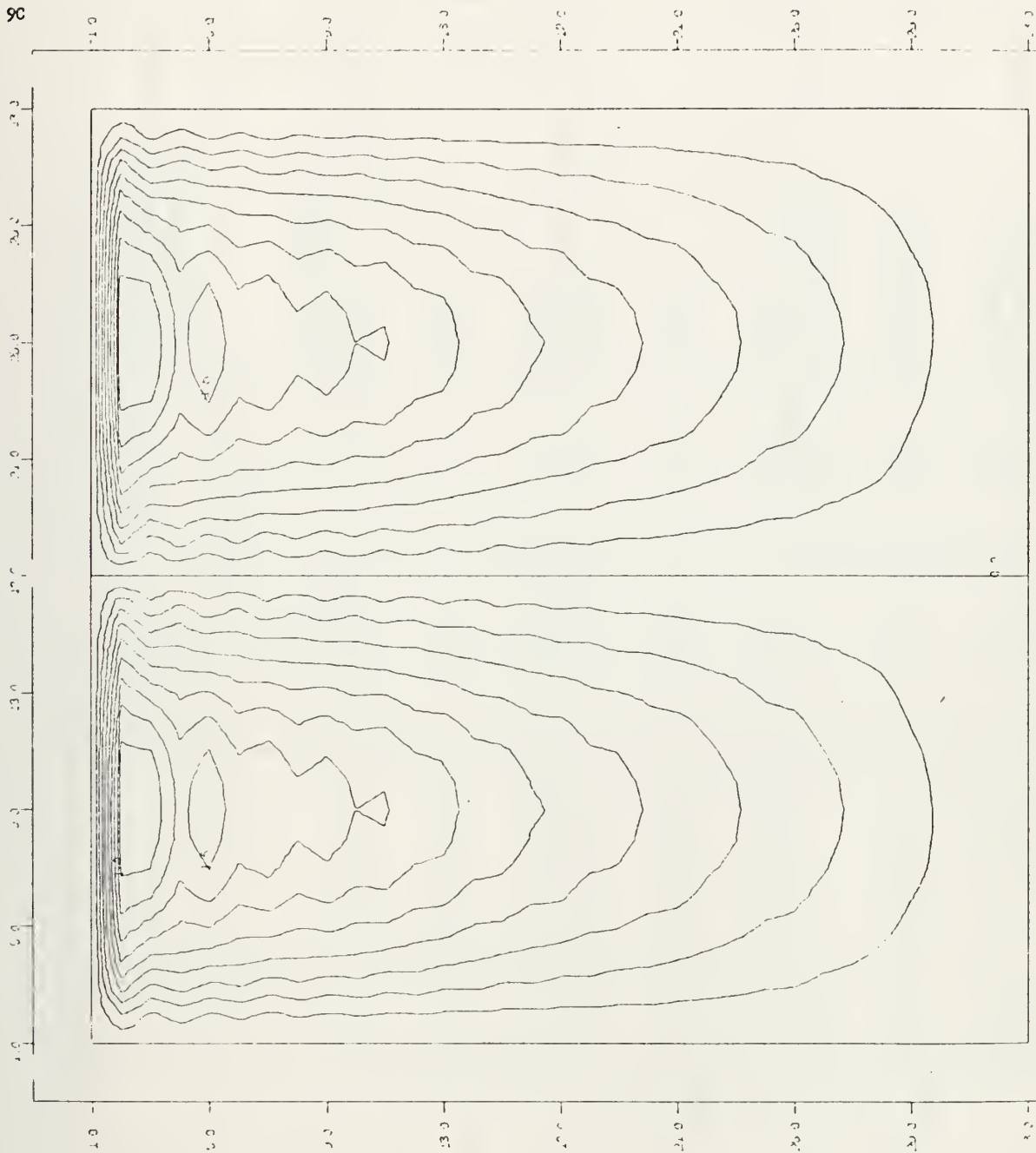


Figure 9C: Numerical Solutions of Ψ for A_1 and $m = 100$, $A \approx |D|$

Figure Number	Type of Solution and B.C.	m	A/A ₁	Ψ_{\max} ($\times 10^8 \frac{\text{cm}^2}{\text{sec}}$)	Location of Ψ_{\max}	Description of Computational Oscillation in Solution of Ψ
4	Analytical $A_1 = \text{const}$	1		2.19 3.72	d/2 d	Very heavy
8A	$A \sim \nabla \zeta $ Symmetrical	10	1.0 to 7.0	3.18	d	Heavy
8B	$A \sim \nabla \zeta $ Extrapolated	10	1.2 to 7.9	3.22	d	Heavy
8C	$A \sim D $	10	1.1 to 10.8	3.09	d	Heavy
9A	$A \sim \nabla \zeta $ Symmetrical	100	1.2 to 41.7	2.31	d	Light
9B	$A \sim \nabla \zeta $ Extrapolated	100	1.3 to 62.2	2.20	d	Light
9C	$A \sim D $	100	1.5 to 70.1	1.98	2d	Light
10A	$A \sim \nabla \zeta $ Symmetrical	1000			2d	Negligible
10B	$A \sim \nabla \zeta $ Extrapolated	1000	1.6 to 237	2.12	2d	Negligible
10C	$A \sim D $	1000	5.0 to 313	2.05	3d	Negligible

TABLE II: Summary of results for significant experiments with non linear coefficient of eddy viscosity $A_{\text{MIN}} = A_1 = .12 \times 10^8 \text{ cm}^2 \text{ sec}^{-1}$.

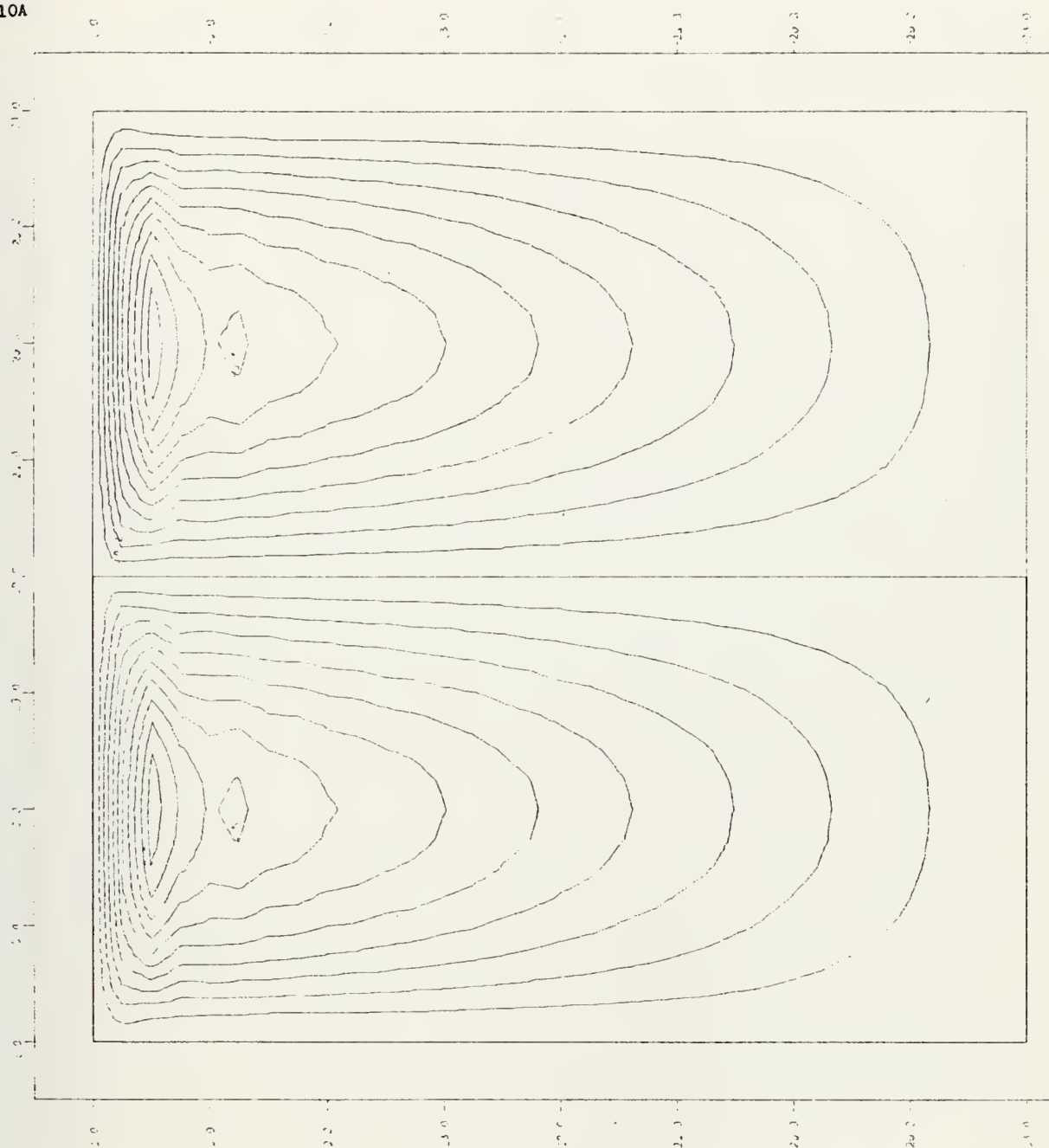


Figure 10A: Numerical Solutions of ψ for Λ_1 and $m = 1000$
Symmetric Boundary Conditions for $\Lambda \sim |\nabla \zeta|$

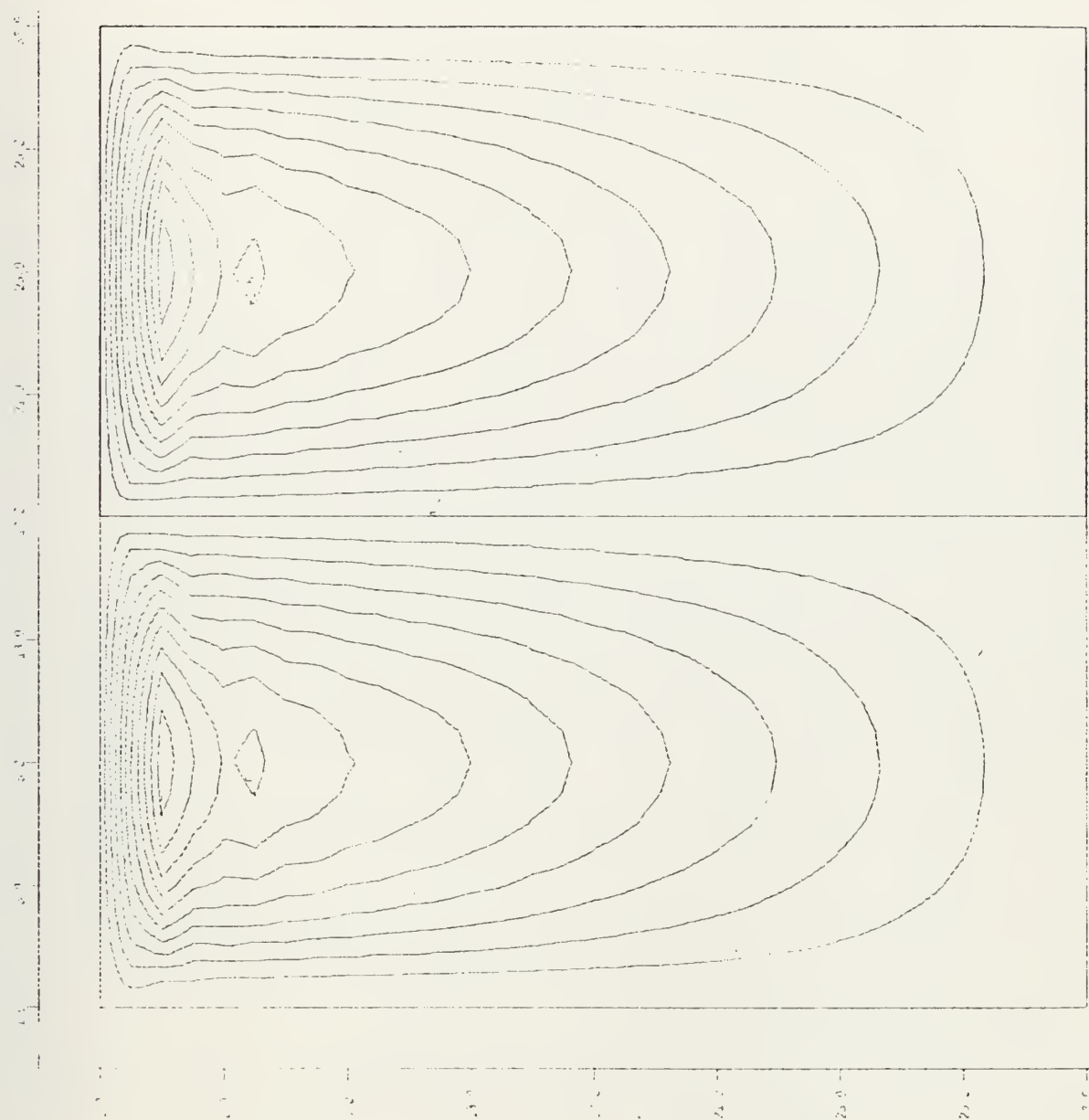


Figure 10B: Numerical Solutions of ψ for Λ_1 and $m = 1000$
 Extrapolated Boundary Conditions for $\Lambda \sim |\nabla \zeta|$

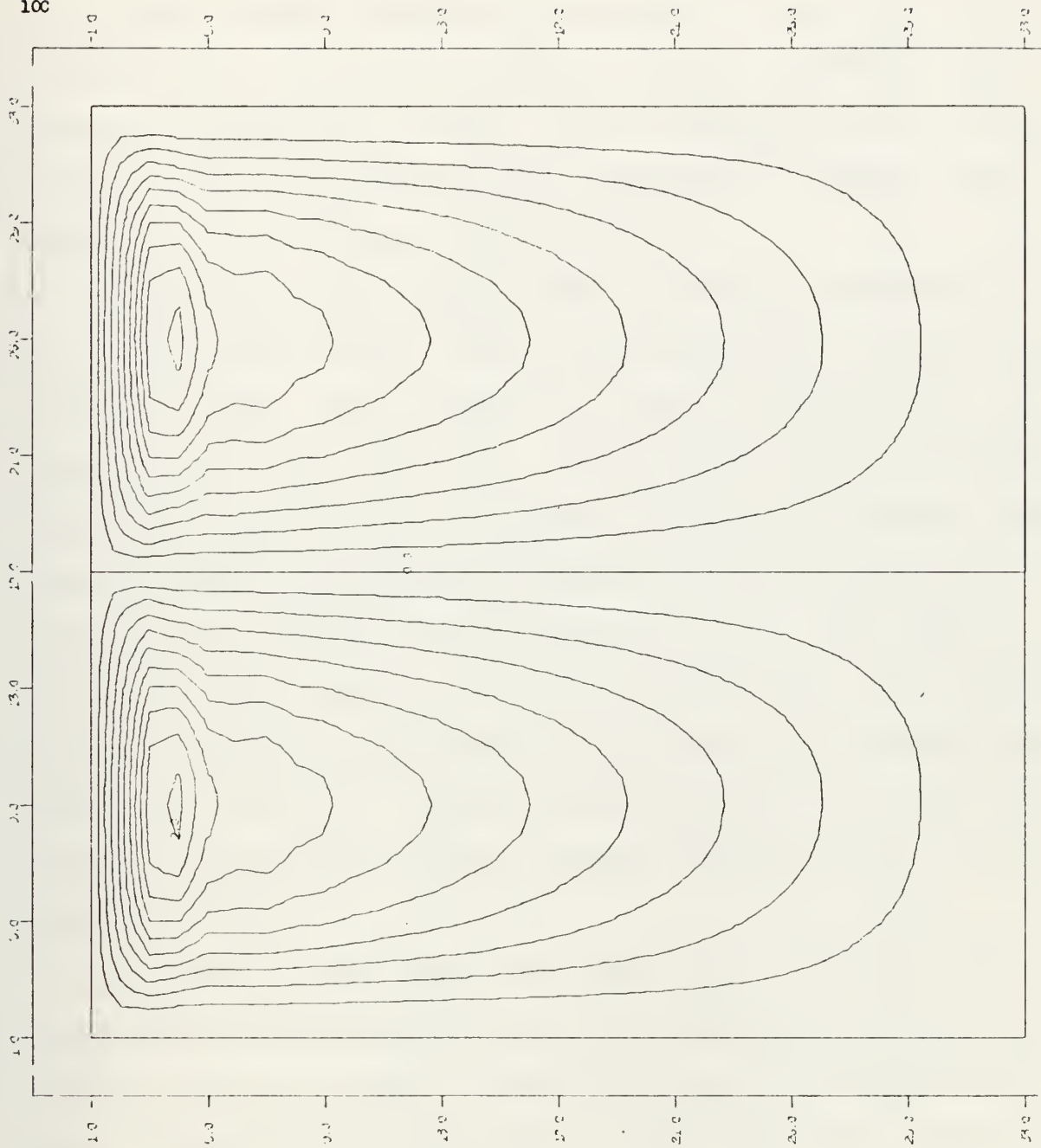


Figure 10C: Numerical Solutions of Ψ for A_1 and $m = 1000$, $A \sim |D|$

move eastward to $3d$ in the case of $A \sim |D|$. Due to this, and the slightly higher minimum coefficients in the ocean interior for the $A \sim |D|$ solution, the $A \sim |\nabla \zeta|$ solution appears to be generally preferred to $A \sim |D|$. This is probably because the method based on two dimensional turbulence is somewhat more sensitive to the space scale of motion.

In the next sets of experiments, $AMIN$ was increased to $A_2 = 0.93 \times 10^8 \text{ cm}^2 \text{ sec}^{-1}$ and m was examined for values ranging from 10 to 100. These results are shown in Figures 11, 12A, 12B, 13, and also Table III. With a higher initial $AMIN$ and resulting higher viscous solution in the ocean interior, the computational oscillation was suppressed and a completely satisfactory solution was attained by $m = 20$. The range of values for A/A_2 and ψ_{\max} are given in Table III, and Figure 11 gives a graphical representation of results for the non linear experiments with A_2 . Increasing m to 100 had the undesirable effect of moving the western boundary eastward to $3d$ in the case of $A \sim |D|$.

Non linear experiments with $AMIN = A_3 = 7.5 \times 10^8 \text{ cm}^2 \text{ sec}^{-1}$ produced no enhancing results. The solution was exceptionally viscous, and the interior ocean was already overdamped with such a high minimum coefficient of eddy viscosity. Increasing m to 10 resulted in moving the ψ_{\max} for $A \sim |D|$ eastward to $3d$. Refer to Table III for representative values of A/A_3 and ψ_{\max} , and to Figure 14 for the streamfunction field for $A \sim |D|$ with $m = 10$.

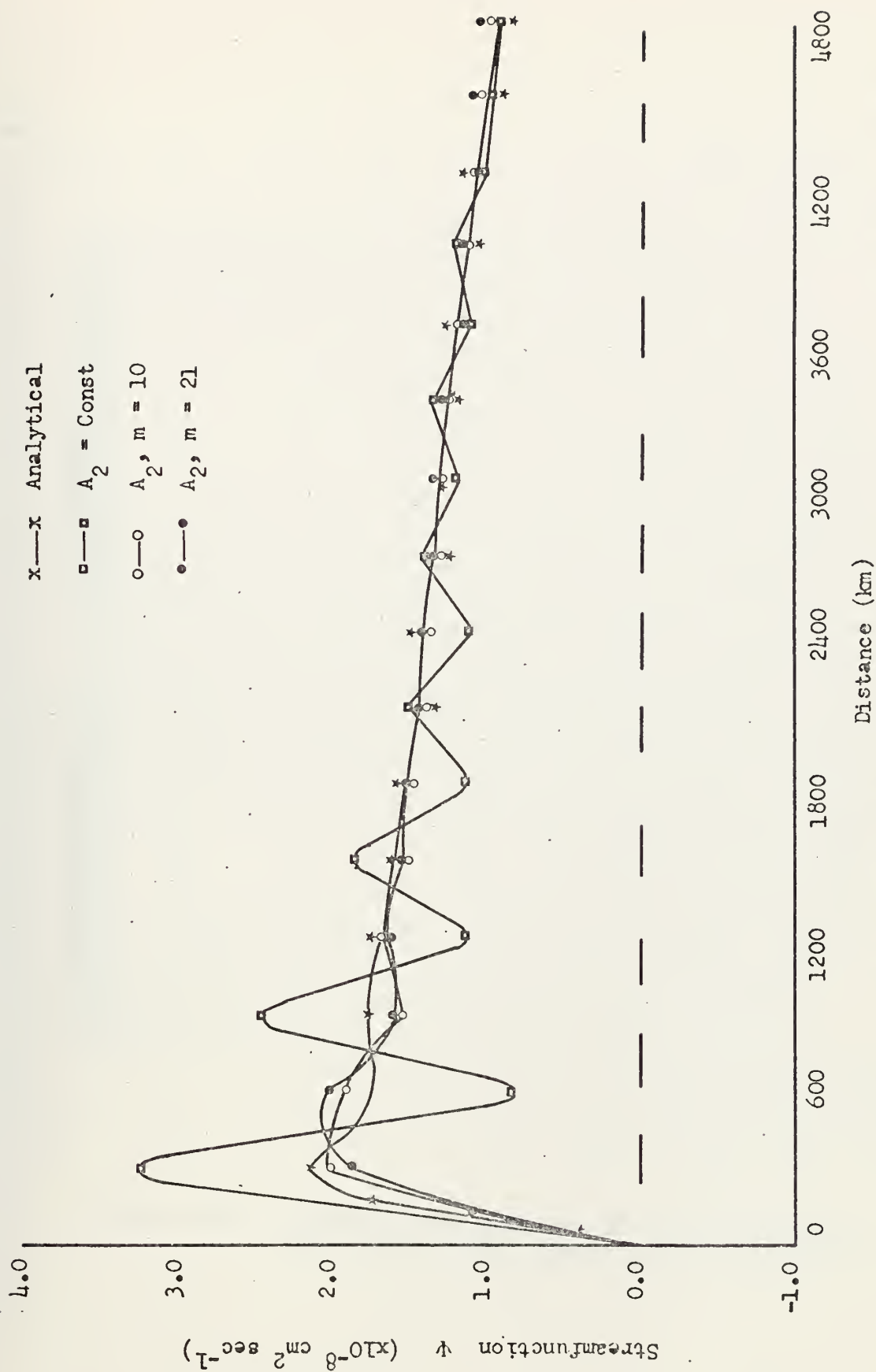


Figure 11: Numerical and Analytical Solutions of ψ at Latitude with Maximum Streamfunction for Non Linear Experiments with A₂, Enstrophy Cascade Case

12A

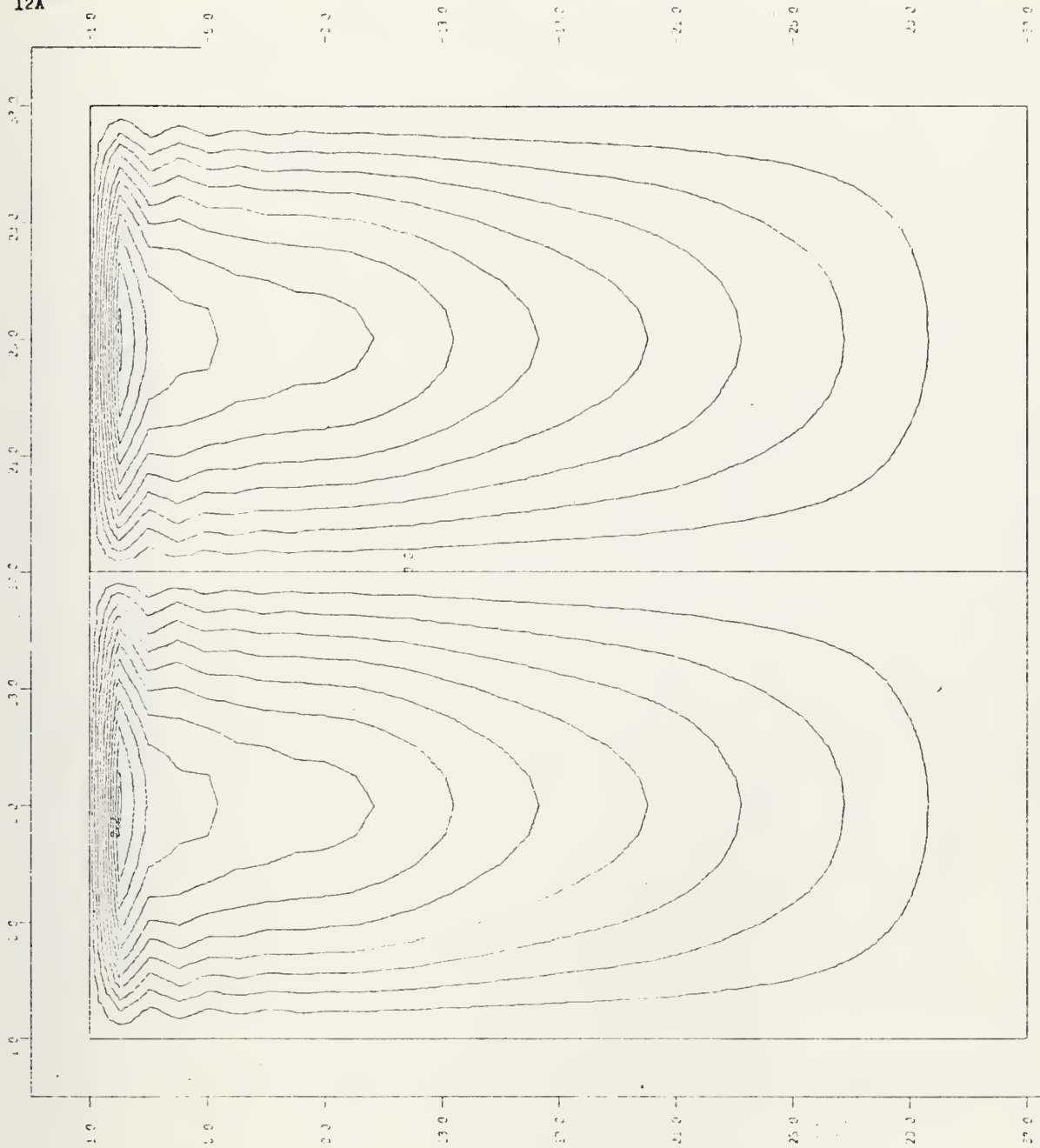


Figure 12A: Numerical Solutions of Ψ for A_2 and $m = 10$
Extrapolated Boundary Conditions for A

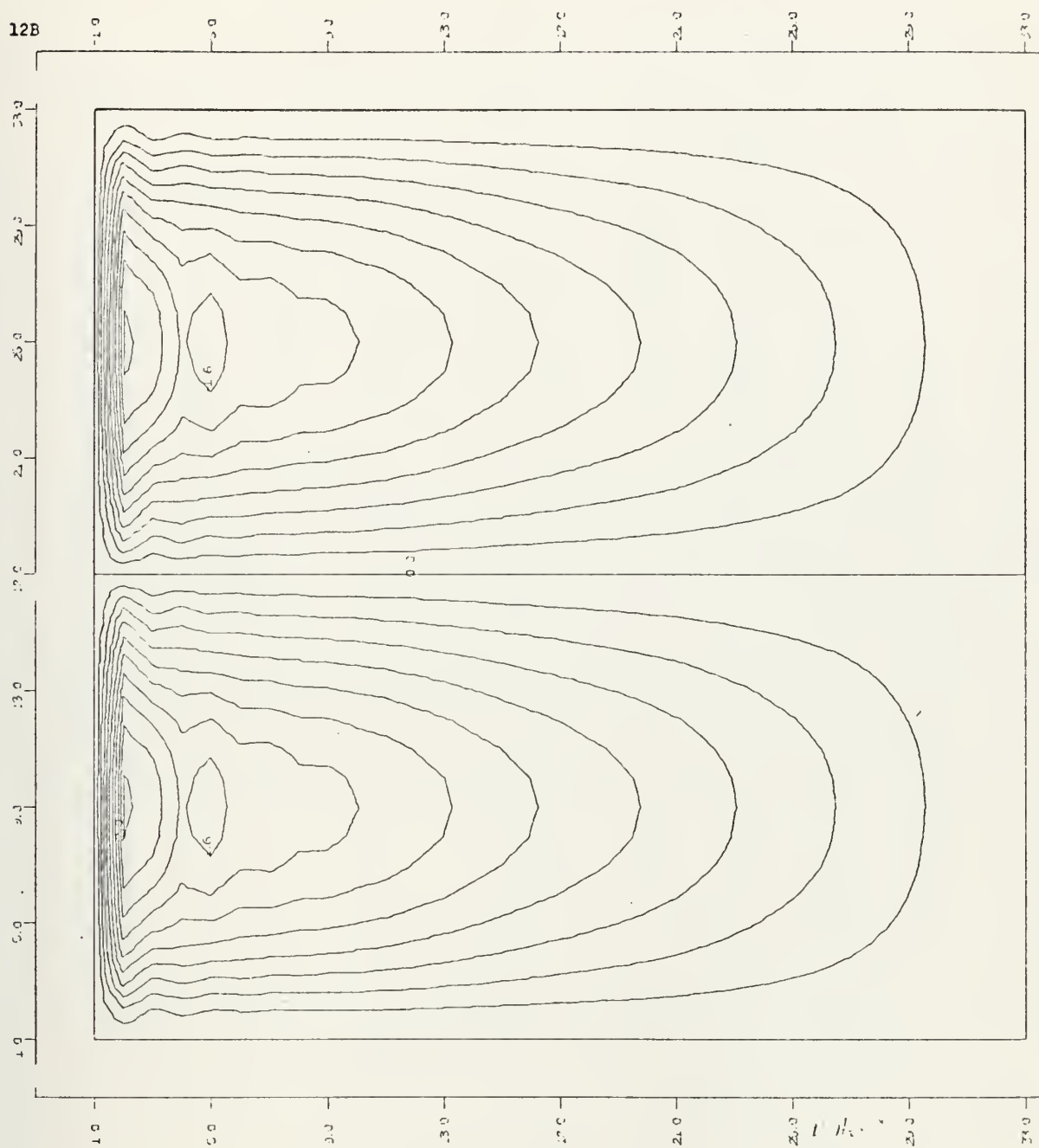


Figure 12B: Numerical Solutions of ψ for A_2 and $m = 10$, $A \sim |D|$

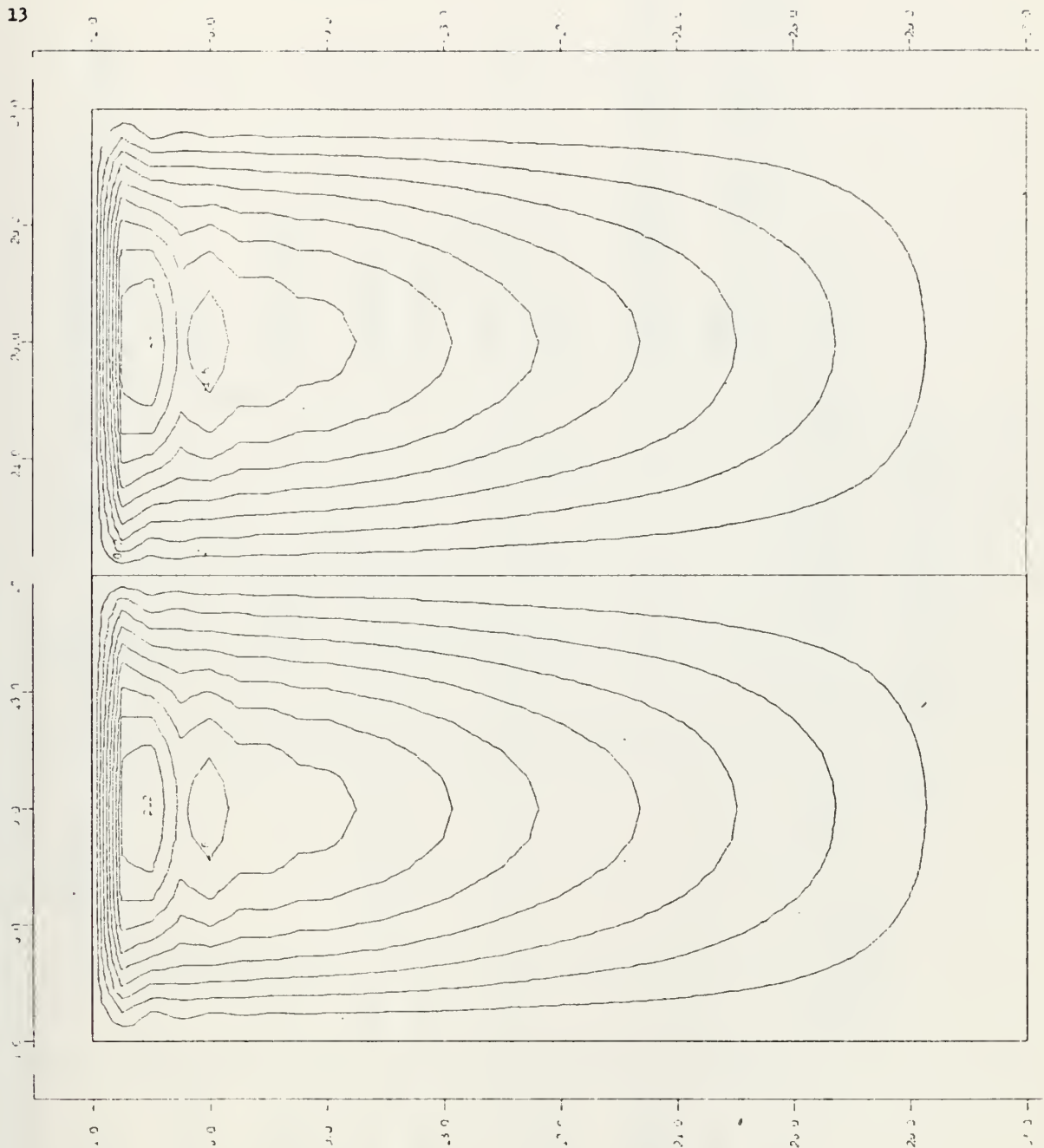


Figure 13: Numerical Solutions of Ψ for Λ_2 and $m = 21$, Extrapolated Boundary Conditions for A

Figure Number	Type of Solution	m	A/AMIN	ψ_{\max} ($\times 10^8 \text{ cm}^2$) sec	Location of ψ_{\max}	Description of Computational Oscillation in Solution of ψ
5	Analytical for A_2			2.17	d	None
	Numerical $A_2 = \text{const}$	1		3.26	d	Moderate
	$A_2, A \sim \nabla \zeta $	10	1.0 to 6.7	2.26	d	Nominal
	$A_2, A \sim D $	10	1.1 to 7.6	2.05	d	Nominal
13	$A_2, A \sim \nabla \zeta $	21	1.0 to 12.0	2.02	2d	Negligible
6	Analytical for A_3			2.13	2d	None
	Numerical $A_3 = \text{const}$	1		2.07	2d	Negligible (very damped interior)
	$A_3, A \sim D $	10	1.0 to 4.1	1.99	3d	None (very damped interior)

TABLE III: Summary of results for significant experiments with non linear coefficients of eddy viscosity AMIN = A_2 and A_3 .

$$A_2 = .93 \times 10^8 \text{ cm}^2 \text{ sec}^{-1}$$

$$A_3 = 7.5 \times 10^8 \text{ cm}^2 \text{ sec}^{-1}$$

The author is of the opinion that the experiment with $AMIN = A_1$ (or perhaps a slightly higher minimum coefficient) and m ranging somewhere between 100 and 1000 (depending on minimum acceptable computational oscillation) gives the best field of non linear lateral eddy viscosity coefficients for future utilization in more sophisticated finite difference ocean circulation models. It appears from the experiments that the only drawback is that these higher values of m produce a western boundary width which is nearly $2d$.

An accurate physical and numerical depiction of both the ocean interior and the western boundary with no computational oscillation was achieved by using either of the two forms of non linear eddy viscosity. These were achieved with the minimum coefficients approximately equal to A_1 in the interior ocean, increasing approximately two orders of magnitude in the more dynamic flow in the western boundary region.

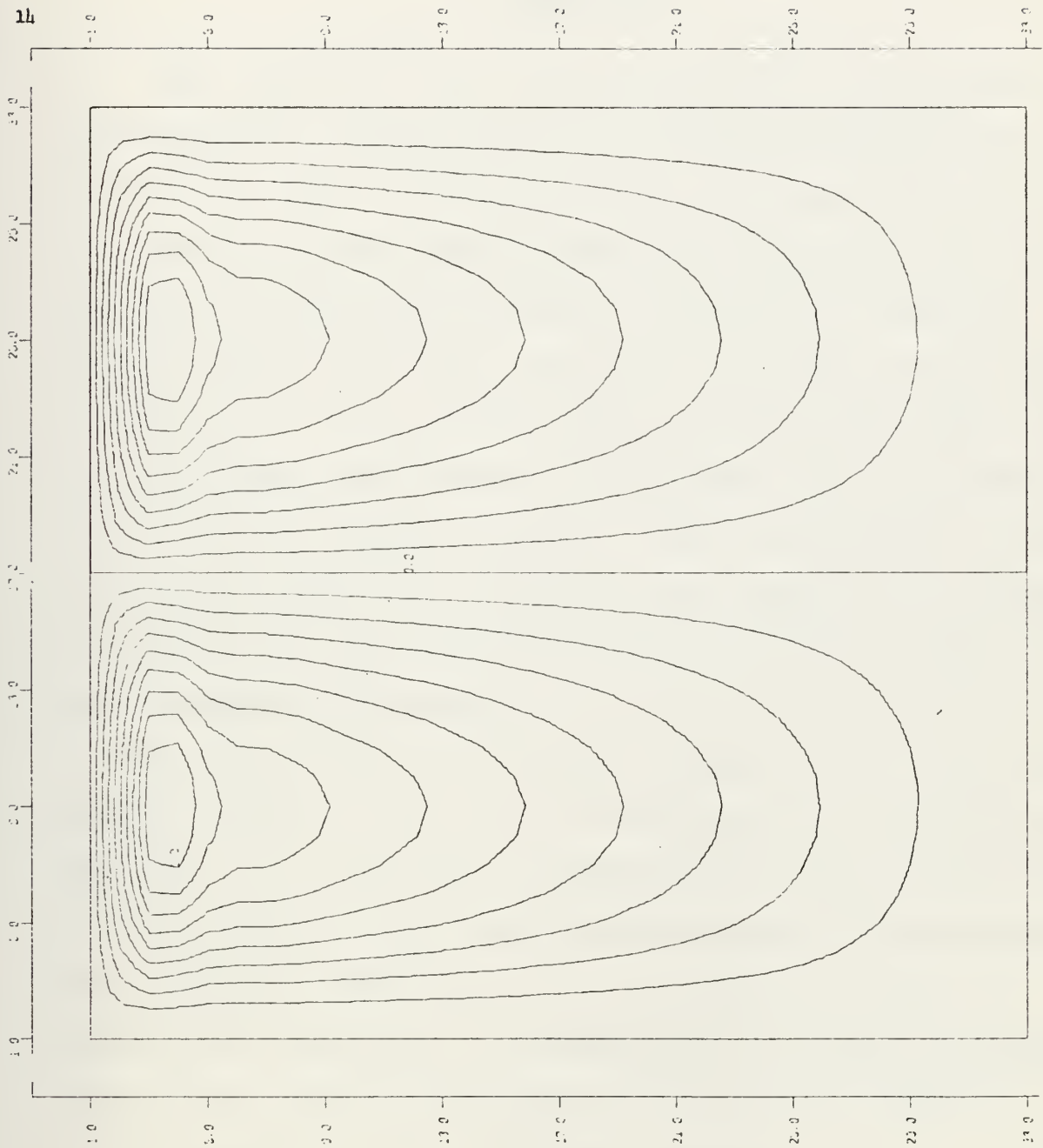


Figure 14: Numerical Solutions of ψ for A_3 and $m = 10$, $A \approx |D|$

V. CONCLUSIONS

This numerical model has been successful in testing a scheme whereby the accuracy of the numerical solution of a finite grid ocean circulation model can be improved by the introduction of non linear lateral eddy viscosity coefficients. Non linear coefficients, properly generated to represent actual physical processes that may be occurring in the ocean, allow the use of low coefficients in the interior ocean solution, and high coefficients in the higher circulation density of the western boundary current. This distribution of eddy viscosity is sufficient to prevent the formation of a computational oscillation which would occur if the low value were used throughout the domain.

Two methods, namely enstrophy cascade ($A \sim |\nabla \zeta|$) and kinetic energy cascade ($A \sim |D|$), were investigated and presented which will allow the researcher to generate non linear coefficients in other models. From experimentation with this barotropic model, minimum coefficients and corresponding ranges of coefficient magnitudes are recommended for initial investigation in more sophisticated baroclinic ocean and coupled ocean-atmosphere finite difference models.

APPENDIX A

LCDR J. M. WRIGHT, JR USN. XM-34, . DEPT OF METEOROLOGY
U. S. NAVAL POSTGRADUATE SCHOOL, MONTEREY, CALIFORNIA
THESIS: OCEAN CIRCULATION MODEL, ONE LEVEL BAPOTROPIC PHASE

THE MAIN PROGRAM INITIATES THE SOLUTION OF THE VORTICITY
EQUATION BY ZEROING ALL DIMENSIONED VARIABLES. THE SUBROUTINES,
NAMELY CALF AND SOLVER, THEN TAKE CONTROL AND PERFORM THEIR
RESPECTIVE FUNCTIONS. AFTERWARD, THE MAIN PROGRAM TAKES CONTROL
AND PERFORMS THE TIME-STEPPING PHASE OF THE SOLUTION.

DVAR MEANS DIMENSIONED VARIABLES *****

COMMON/ JVAR/ PSI, F1, U, V, DELSQ, DELSQV, DPSIDT, RESID, PSTEMP, A
COMMON/ DCMAIN/ IM, JM, IMM1, JMM1, IMP1, JMP1, K, KK, AMIN, DEF
DIMENSION PSI(33,33), PSI(33,33), F1(33,33), U(34,34), V(34,34),
1 DELSQ(32,32), DELSQV(32,32), DPSIDT(33,33), RESID(34,34),
2 PSTEMP(33,33), DATA1(33,33), A(34,34), DEF(33,33)

REAL*8 TITLE(12)

REAL*4 CL(41)

LOGICAL*1 LTG(3)/.TRUE.,.TRUE.,.FALSE./

IM=33

JM=33

IMM1=32

JMM1=32

IMP1=34

JMP1=34

CL(1)=-4.0

DO 10 N=2,41

10 CL(N)=CL(N-1)+0.2

START THE ZEROING PROCESS.

DO 3000 J=1,JM

DO 3000 I=1,IM

PSI(I,J)=0.0

PSI(I,J)=0.0

F1(I,J)=0.0

RESID(I,J)=0.0

PSTEMP(I,J)=0.0

3000 DPSIDT(I,J)=0.0

DO 4000 J=1,JMM1

DO 4000 I=1,IMM1

DELSQV(I,J)=0.0

4000 DELSQ(I,J)=0.0

DO 5000 J=1,JMP1

DO 5000 I=1,IMP1

A(I,J)=0.0

U(I,J)=0.0

5000 V(I,J)=0.0

KK=0

MATSUMO SCHEME IS USED FOR THE FIRST TIME STEP, AND EVERY 50 TIME
STEPS THEREAFTER

MATSNJ=5)

DELTAX=3.0 * 10.0**7

DELTAT= 5.0 * 10.0**4

TIMEST=210.0*86400.)

TIME=0.0

LEAPFROG TIME SCHEME *****

THE LEAPFROG SCHEME IS NEUTRAL IN CHARACTER BUT THE PRESENCE AND


```

C      UTILIZATION OF THREE TIME LEVELS IN THE DESCRIPTION OF THE FIRST
C      DERIVATIVE OF PSI WITH RESPECT TO TIME , PRODUCES A COMPUTATION-
C      AL MODE IN TIME. THIS MODE HAS TO BE AND IS REMOVED BY THE EULER-
C      BACKWARD SCHEME. THIS SCHEME USES TWO LEVELS IN TIME IN ITS DE-
C      SCRIPTON OF THE FIRST TIME DERIVATIVE OF PSI. THEREFORE, THERE
C      IS NO COMPUTATIONAL MODE IN TIME AND A MORE ACCURATE SOLUTION
C      FOR THE PSI FIELD AT TIME LEVEL 'N+1' IS ATTAINED . *****
C
C      DO 3100 K=1,3000
C      IF (K.EQ.1) GO TO 2000
C      L=MOD(K,MATSNQ)
C      IF (L.EQ.0) GO TO 2000
C      CALL CALF
C      CALL SOLVER(DPSIDT,IMM1,JMM1,DELTAX,DELTAX)
C      DO 6000 J=2,JMM1
C      DO 6000 I=2,IMM1
C      TEMP=PSI(I,J)
C      PSI(I,J)= PSIM1(I,J)+2.0 * DELTAT * DPSIDT(I,J)
6000  PSIM1(I,J) = TEMP
C
C      PRINT THE PSI FIELD IN TABULAR FORM *****
C
C      GO TO 2300
C
C      AT THIS TIME , PSI IS KNOWN AT TWO CONSEQUETIVE TIME LEVELS AND
C      IS STORED IN PSI AND PSIM1 FIELDS RESPECTIVELY. BY MEANS OF THE
C      TEMP STATEMENT , THE TWO TIME LEVELS ARE ADVANCED BY ONE INCRE-
C      MENT OF TIME , I.E., DELTAT = 5.0 *10.0**4 (SEC.) RESPECTIVELY.
C
C      THE EULER-BACKWARD OR MATSUNO TIME SCHEME ; NOTE: PSI AT TIME
C      LEVEL 'N' IS SAVED IN PSTEMP FIELD FOR LATER USE IN SUBSEQUENT
C      BACKWARD IMPLICIT STEP . *****
C
C      2000 WRITE(6,103) TIME
C      2100 DO 2200 J=2,JMM1
C      DO 2200 I=2,IMM1
C      PSIM1(I,J)=PSI(I,J)
2200  PSTEMP(I,J)=PSI(I,J)
C
C      BY MEANS OF THE ABOVE LOOP(#2200), PSI AT TIME LEVEL N IS PUT IN-
C      TO THREE FIELDS , NAMELY PSI, PSTEMP AND PSIM1. ALL FIELDS ARE AT
C      THE SAME TIME LEVEL IN ORDER TO PRESERVE LINEAR COMPUTATIONAL
C      STABILITY IN THE FRICTION TERM OF THE FORCING FUNCTION, F1. *****
C
C      COMMENCE THE FORWARD TIME STEP PHASE OF THE MATSUNO SCHEME. ****
C
C      NOTE: ALL TERMS OF CALF AND RELAX ARE OUTPUTED AT TIME LEVEL N .
C
C      CALL CALF
C      SCALE=10.0**(-2)
C      DO 2910 J=2,JMM1
C      JS=JMP1-J
C      DO 2910 I=2,IMM1
2910  RESID(I,J)=F1(I,JS)*SCALE
C      WRITE(6,108) ((RESID(I,J),I=2,32),J=2,32)
108  FORMAT('0','RESID FIELD = F1 FIELD * SCALE',/,31(1X,31F4
1.2,///))
C      CALL SOLVER(DPSIDT,IMM1,JMM1,DELTAX,DELTAX)
C
C      DPSIDT IS NOW AT TIME LEVEL 'N' . *****
C
C      DO 2500 J=2,JMM1
C      DO 2500 I=2,IMM1
C      PSI(I,J)= PSI(I,J) + DELTAT * DPSIDT(I,J)
2500  PSIM1(I,J)=PSI(I,J)
C
C      PRESENTLY, THE FIELDS PSI, PSIM1 AND PSTEMP HAVE CONTAINED IN **
C      THEM , PSI VALUES AT TIME LEVELS 'N+1' INTERMEDIATE , 'N+1' INTER-

```



```

C      MEDIATE AND 'N' RESPECTIVELY. *****
C
C      NOW AS A PART OF THE MATSUNO TIME SCHEME ; A SIMULATED (IMPLICIT
C      E) BACKWARD TIME STEP IS EMPLOYED. THE BACKWARD STEP IS USED AS
C      A CALIBRATION STEP TO REFINED THE PSI FIELD AT TIME LEVEL 'N+1'.
C      COMMENCE THE BACKWARD TIME STEP PHASE OF THE MATSUNO SCHEME. **
C      NOTE: ALL TERMS OF CALF CALCULATED AS A FUNCTION OF PSI AT INTER-
C      MEDIATE TIME LEVEL 'N+1'. *****
C
C      CALL CALF
C      CALL SOLVER(DPSIDT,IMM1,JMM1,DELTAX,DELTAX)
C
C      DPSIDT AT TIME LEVEL 'N+1' (INTERMEDIATE) OUTPUTED. *****
C      NOW OUTPUT PSI AT TIME LEVEL 'N+1'. *****
C
C      DO 2700 J=2,JMM1
C      DO 2700 I=2,IMM1
C      PSIM1(I,J)=PSTEMP(I,J)
2700  PSI(I,J)=PSTEMP(I,J) + DELTAT * DPSIDT(I,J)
2800  TIME=DELTAT*K
C      WRITE(6,103) TIME,K
C      SCALE= 10.0*(-8)
C
C      PRINT OUT 'A' FIELD DERIVED FROM DEFORMATION
C
C      DO 1140 J=1,JMP1
C      JS=JM+2-J
C      DO 1140 I=1,IMP1
1140  RESID(I,J)=A(I,JS)/AMIN
C      IF (MOD(K,20).EQ.0)
C      @WRITE (6,1145)((RESID(I,J),I=1,33),J=1,34)
C
C      1145  FORMAT('0','RESID FIELD = A FIELD/AMIN',/,34(1X,33F4.0,//))
C      DO 2900 J=1,JM
C      JS=JMP1-J
C      DO 2900 I=1,IM
2900  RESID(I,J)= PSI(I,JS) * SCALE
C      IF (MOD(K,20).EQ.0)
C      @WRITE(6,104) ((RESID(I,J),I=1,33),J=1,33)
103  FORMAT(' ',T63,'TIME=',F10.1,I6,//)
104  FORMAT('0','RESID FIELD = PSI FIELD * SCALE',/,33(1X,33F4.2,//))
C      LL=MOD(K,3)
C      TDAY=TIME/86400.0
C      WRITE(6,103) TDAY,LL
C
C      LCCP IS FOR THE CONVERSION OF DATA TO A FORM MORE USEABLE IN 'CC
C      -TUR' *****
C
C      DO 2950 J=1,JM
C      DO 2950 I=1,IM
2950  DATA1(I,J)=PSI(I,J)*SCALE
C      IF((TDAY.GT.202.0).AND.(LL.EQ.0)) GO TO 9970
C      GO TO 9980
9970  REAL(5,9999) (TITLE1(J),J=1,12)
9999  FORMAT(6A8)
C      CALL CCNTUR(DATA1,33,33,33,CL,41,TITLE1,8,08,LTG)
9980  IF(TIME.GE.TIMEST) STOP
3100  CONTINUE
C      STCP
C      DEBUG
C      AT 3100
C      TRACE ON
C      DISPLAY K
C      END

```



```

C
C
C
C
C
C
SUBROUTINE CALF
THIS SUBROUTINE CALCULATES THE RIGHT HAND SIDE OF THE VORTICITY
EQUATION WHICH IS MULTIPLIED BY THE SQUARE OF DELTAX.
DVAR      MEANS  DIMENSIONED VARIABLES      *****
COMMON/DVAR/PSIM1,PSI,F1,U,V,DELSQU,DELSQV,DPSIDT,RESID,PSTEMP,A
COMMON/DOMAIN/IM,JM,IMM1,JMM1,IMP1,JMP1,K,KK,AMIN,DEF
DIMENSION PSIM1(33,33),PSI(33,33),F1(33,33),U(34,34),V(34,34),
1DELSQU(32,32),DELSQV(32,32),DPSIDT(33,33),RESID(34,34),
2PSTEMP(33,33),PSIANL(100),DEF(33,33),DEFS(33,33),DEFT(33,33)
DIMENSION DELVOP(33,33),A(34,34)
DIMENSION FX(33,33),FY(33,33),GX(33,33),GY(33,33),UT(33,33),VT(33,
33),UAV(34,34),VAV(34,34),VORT(33,33),UAVE(34,34),VAVE(34,34)
DIMENSION PSIX(35,35),VORTX(33,33)
DIMENSION VORT1(33,33),VORT2(33,33),VORT3(33,33)
C
C
C
BETA TERM CALCULATION, A/BETA CONSISTENT WITH NORPAX MODEL
PI=3.1415926
OMEGA=2.*PI/86400.
RAD=6.375*10.**8
BETA=(2.0*OMEGA/RAD)*65./90.
DELTAX=3.*10.**7
C
C
C
WL=WIDTH OF WESTERN BOUNDARY; WL1=DELTAX/2; UNSTABLE CASE
WL1=DELTAX/2.
ALFA=BETA*((SQRT(3.)/(2.*PI))*WL1)**3)
AMIN=ALFA
IF (KK.EQ.0) WRITE(6,28) ALFA
28  FORMAT(/,1X,'ALFA =',E12.4)
DX=DY FOR THIS MODEL
DELTAY=3.*10.**7
C
C
C
CUP=.5
DO 30 J=2,JMM1
DO 30 I=2,IMM1
30  F1(I,J) = -(BETA)*(CUP*(PSI(I+1,J)-PSI(I,J))+(1.-CUP)*(PSI(I,J)-
@PSI(I-1,J)))*DELTAX
C
C
C
C
C
C
STRESS CURL TERM CALCULATION *****
THE AMOUNT OF POSITIVE VORTICITY INTO THE OCEAN FROM THE ATMOSPHERE
IS NEGATIVE ( ANTI-CYCLONIC ). THIS MAKES THE OCEAN SPIN A/C LIKE A
HIGH,PRODUCING A POSITIVE STREAMFUNCTION, PSI.
F=1.0
DEPTH=2.0*10.0**5
FJMM1=JMM1
B=FJMM1*DELTAX
DO 40 J=2,JMM1
Y=PI*(J-1)*(1.0/B)*DELTAX
STRESS= ((2.*F*PI) / (DEPTH*3)) * SIN(2.*Y)
DO 40 I=2,IMM1
40  F1(I,J)=F1(I,J)-(STRESS *DELTAX **2)
C
C
C
C
C
C
DETERMINATION OF PSI FIELD BY ANALYTICAL MEANS. PRINT OUT MAX
ANALYTIC PSI FIELD WHICH OCCURS AT ROW J=9.
KK=KK+1
IF(KK.GE.2) GO TO 43
PSIANL =-R * X(X) * BETA**(-U) * CURL (TAU) = ANALYTICAL PSI FIELD
R = DOMAIN WIDTH
FIMM1=IMM1
R=FIMM1*(DELTAX)
BETA = DF/DY (AS ABOVE)
CURL (TAU) = K COMPONENT OF WIND STRESS CURL = STRESS (AS ABOVE)
X(X) = XX. SEE MUNK (1951, EQ. 20):
XX=HKK*(EXP(-1/2*HK*X))*COS(((SQRT 3)/2)*HK*X+(SQRT 3)/(2*HK*R) -

```



```

C      PI/6)+1-(1/(HK*R))*(HK*X-EXP(-HK*(R-X))-1), WHERE
      HK=(BETA/ALFA)**.33333333
      HKK=2./SQRT(3.)-SQRT(3.)/(HK*R)
      Y=PI*3.*(1./B)*DELTA
      STRESS=-((2.*PI)/(DEPTH*B))*SIN(2.*Y)
      J=9
C      FOR EXPANDED ANALYTICAL SOLUTION, DELTAX DECREASED BY ORDER OF 10
C      DELTAX NOW EQUAL 30 KM; WILL EXAMINE WESTERN 1/3 OF OCEAN
      DELTAX=3.*10.**6
      DO 42 I=1,100
      X=(I-1)*DELTA
      XX=-HKK*(EXP(-.5*HK*X))*COS(((SQRT(3.))/2.)*HK*X+((SQRT(3.))/(2.*HK
      @*R)-PI/6.))+1-(1/(HK*R))*(HK*X-EXP(-HK*(R-X))-1.)
      PSIANL(I)=-R*XX*BETA*(-1)*STRESS
C      NORMALIZE PSIANL FIELD BY DIVIDING BY PSIANL MAX
      PSIANL(I)=PSIANL(I)/(10.**8)
      42 IF ((MOD(K,20).EQ.0).OR.(KK.EQ.1))
      @WRITE(6,44) (PSIANL(I),I=1,99)
      44 FORMAT('0', 'THE MAX ANALYTIC PSI FIELD IS FOR ROW J=9:',/,1X,33F4.
      @2,/,1X,33F4.2,/,1X,33F4.2,/)
      DELTAX=3.*10.**7

```

CALCULATION OF FRICTION TERM USING PSIM1 (FORWARD TIME SCHEME) *

FRICTION TERMS ARE CALCULATED USING A FORWARD TIME SCHEME. THIS IS DONE TO PRESERVE LINEAR COMPUTATIONAL STABILITY. IF THE LEAP FRG SCHEME WAS UTILIZED, THE FRICTION TERM WOULD BE UNSTABLE.

DEFINE INITIAL U(32,32) AND V(32,32) AS FUNCTIONS OF PSIM1(33,33) REFERENCE SHOULD BE MADE TO SKETCH OF GRID IN NOTES: ***** U(I+1,J+1) AND V(I+1,J+1) TRANSFORM U,V(32,32) INTERNAL GRID ** SYSTEM INTO EXTERNAL U,V(34,34) GRID SYSTEM *****

```

49 DO 50 I=1,IMM1
DO 50 J=1,JMM1
AA= PSIM1(I+1,J+1) + PSIM1(I+1,J)
BB= PSIM1(I,J+1) + PSIM1(I,J)
CC= PSIM1(I+1,J+1) +PSIM1(I,J+1)
DD= PSIM1(I+1,J) + PSIM1(I,J)
EE = 2.0*DELTA
V(I+1,J+1) = ((AA/EE) -(BB/EE))
50 U(I+1,J+1) = ((DD/EE) -(CC/EE))

```

DEFINE EXTERNAL BOUNDARY VALUES OF U AND V *****

```

DO 60 I=2,IM
U(1,1) = -U(1,2)
V(1,1) = -V(1,2)
U(1,JMP1)=-U(1,JM)
60 V(1,JMP1)=-V(1,JM)
DO 70 J=2,JM
U(1,J)=-U(2,J)
V(1,J)=-V(2,J)
U(IMPL,J)=-U(IM,J)
70 V(IMPL,J)=-V(IM,J)
U(1,1)=U(2,2)
V(1,1)=V(2,2)
U(34,34)=U(33,33)
V(34,34)=V(33,33)
U(1,34)=U(2,33)
V(1,34)=V(2,33)
U(34,1)=U(33,2)
V(34,1)=V(33,2)
IF(KK.GE.0) GO TO 3100

```

CALCULATION OF THE FIELD VARIABLE OF COEFFICIENTS OF EDDY VISCOSITY 'A,' BASED ON ENSTROPY CASCADE

VORT(I,J) IS THE RELATIVE VORTICITY AT EACH GRID POINT.


```

C
1101 DO 1105 I=1,IM
      DO 1105 J=1,JMP1
1105  UAV(I,J)=(U(I,J)+U(I+1,J))/2.
      DO 1110 I=1,IMPI
      DO 1110 J=1,JM
1110  VAV(I,J)=(V(I,J)+V(I,J+1))/2.
C    VORTICITY(I,J)=DV/DX - DU/DY
      DO 1115 I=1,IM
      DO 1115 J=1,JM
1115  VORT(I,J)=(VAV(I+1,J) - VAV(I,J))/DELTA X - (UAV(I,J+1) - UAV(I,J))
      @/DELTA Y
C
      IF (K.GE.0) GO TO 1120
C
C    EXAMINING VARIOUS METHODS OF COMPUTING VORTICITY FROM K. MIYOKUDA
C    "NUMERICAL WEATHER PREDICTION, COMPUTATIONAL METHODS," 1962.
C
C    SETTING UP AN EQUIVALENT 35X35 PSI FIELD: PSIX(I,J)
C
      DO 1121 I=2,34
      DO 1121 J=2,34
1121  PSIX(I,J)=PSI(I-1,J-1)
      DO 1122 J=2,34
      PSIX(1,J)=PSIX(3,J)
1122  PSIX(35,J)=PSIX(33,J)
      DO 1123 I=2,34
      PSIX(I,1)=PSIX(I,3)
1123  PSIX(I,35)=PSIX(I,33)
      PSIX(1,1)=PSIX(3,3)
      PSIX(1,35)=PSIX(3,33)
      PSIX(35,1)=PSIX(33,3)
      PSIX(35,35)=PSIX(33,33)
C
C    ORIGINAL EQUIVALENT 'X' METHOD, USES 5 GRIDPOINTS:
C
      DO 1124 I=2,34
      DO 1124 J=2,34
1124  VORTX(I-1,J-1)=.5*(PSIX(I-1,J+1)+PSIX(I+1,J+1)+PSIX(I+1,J-1)+
      &PSIX(I-1,J-1)-4.*(PSIX(I,J)))/(DELTA X**2)
C
C    MIYAKODA METHOD I, 'MINIMUM GRIDPOINT' SCHEME, VORT+=VORT1, USES
C    5 GRIDPOINTS
C
      DO 1125 I=2,34
      DO 1125 J=2,34
1125  VORT1(I-1,J-1)=.5*(PSIX(I-1,J)+PSIX(I,J+1)+PSIX(I+1,J)+PSIX(I-1,J
      &)-4.*(PSIX(I,J)))/(DELTA X**2)
C
C    MIYAKODA METHOD II, "ORIENTATIONAL MINIMUM ERROR," VORT2=(2*VORT1+
C    1*VORTX)/3; USES 9 GRIDPOINTS TO SOLVE FOR VORTICITY
C
      DO 1126 I=1,33
      DO 1126 J=1,33
1126  VORT2(I,J)=(2.*VORT1(I,J)+VORTX(I,J))/3.
C
C    MIYAKODA METHOD III, "KNIGHTING & OGURA" SCHEME: (2*VORT1-VORTX)/3
C
      DO 1127 I=1,33
      DO 1127 J=1,33
1127  VORT3(I,J)=(2.*VORT1(I,J) - VORTX(I,J))
C
1128 DO 1129 I=1,33
      DO 1129 J=1,33
1129  VORT(I,J)=VORT3(I,J)
1120 CONTINUE
C
C    DETERMINING A VARIABLE LATERAL COEFFICIENT OF EDDY VISCOSITY, 'A',
C    BASED ON ENSTROPY CASCADE
C
      DO 1130 I=2,IM
      DO 1130 J=2,JM
1130  DELVOR(I,J)=SQRT(ABS((((VORT(I,J)+VORT(I,J-1))/2.-(VORT(I-1,J)+VOR

```



```

      DT((I-1,J-1))/2.)/DELTAX)**2+(((VORT(I,J)+VORT(I-1,J))/2.-(VORT(I,J-
      #1)+VORT(I-1,J-1))/2.)/DELTAX)**2))
      DVCRMV=2.*(10.**(-6))/DELTAX
      DO 1135 I=2,IM
      DO 1135 J=2,JM
C
1135 A(I,J)= AMIN*(1.+999.*DELVOR(I,J)/DVORMV)
C
      IF(KK.GE.0) GO TO 1160
C
      BOUNDARY VALUES FOR ENSTROPHIC A (34,34): LINEAR EXTRAPOLATIONS
C
      IN ALL FOUR DIRECTIONS
C
      DO 1150 I=2,IM
      SLCPE=(A(I,2)-A(I,3))/DELTAY
      A(I,1)=(SLCPE*DELTAY)+A(I,2)
      SLCPE=(A(I,JM)-A(I,JM1))/DELTAY
1150 A(I,JM1)=(SLCPE*DELTAY)+A(I,JM)
      DO 1155 J=2,JM
      SLCPE=(A(2,J)-A(3,J))/DELTAX
      A(1,J)=(SLCPE*DELTAX)+A(2,J)
      SLCPE=(A(IM,J)-A(IM+1,J))/DELTAX
1155 A(IM+1,J)=(SLCPE*DELTAX)+A(IM,J)
C
1160 CONTINUE
C
      METHOD 2 FOR DETERMINING BOUNDARY CONDITIONS FOR ENSTROPHIC A,
C
      (34,34): EXTENSION OUTWARD OF EXISTING INTERIOR BOUNDARIES.
C
      DO 1165 J=2,JM
      A(1,J)=A(2,J)
1165 A(IM+1,J)=A(IM,J)
      DO 1170 I=2,IM
      A(I,1)=A(I,2)
1170 A(I,JM1)=A(I,JM)
C
C
      FX=D/DX(A DU/DX) + D/DY(A DV/DY)
C
      FY=D/DX(A DV/DX) + D/DY(A DU/DY)
C
      DO 1205 I=2,IM
      DO 1205 J=2,JM
      FX(I,J)=(((A(I,J)+A(I+1,J))/2.)*(U(I+1,J)-U(I,J)) -
      2*((A(I-1,J)+A(I,J))/2.)*(U(I,J)-U(I-1,J))+
      3*((A(I,J)+A(I,J+1))/2.)*(U(I,J+1)-U(I,J)) -
      4*((A(I,J-1)+A(I,J))/2.)*(U(I,J)-U(I,J-1)))
C
      FY(I,J)=(((A(I,J)+A(I+1,J))/2.)*(V(I+1,J)-V(I,J)) -
      2*((A(I-1,J)+A(I,J))/2.)*(V(I,J)-V(I-1,J))+
      3*((A(I,J)+A(I,J+1))/2.)*(V(I,J+1)-V(I,J)) -
      4*((A(I,J-1)+A(I,J))/2.)*(V(I,J)-V(I,J-1)))
1205 CONTINUE
3100 CONTINUE
C
      CALCULATION OF THE FIELD VARIABLE OF COEFFICIENTS OF EDDY VISCOSITY
      'A,' BASED ON KINETIC ENERGY CASCADE
C
      FOR KINETIC ENERGY CASCADE, DEFORMATION ALONG A STREAMLINE, DEFS =
C
      DV/DX + DU/DY. DEFORMATION NORMAL TO A STREAMLINE, DEFT = DU/DX -
C
      DV/DY. ABSOLUTE VALUE OF DEFORMATION, DEF(I,J) = SQRT(DEFS**2 +
C
      DEFT**2).
C
3101 DO 3105 I=1,IM
      DO 3105 J=1,JM1
      VAVE(I,J)=(V(I,J)+V(I+1,J))/2.
3105 UAVE(I,J)=(U(I,J)+U(I+1,J))/2.
      DO 3110 I=1,IM1
      DO 3110 J=1,JM
      UAVE(I,J)=(U(I,J)+U(I,J+1))/2.
3110 VAV(I,J)=(V(I,J)+V(I,J+1))/2.
C
      VAV USED IN DV/DX, UAV USED IN DU/DY, VAVE USED IN DV/DY,
C
      UAVE USED IN DU/DX
C
      DO 3115 I=1,IM
      DO 3115 J=1,JM

```



```

      DEFS(I,J)=(VAV(I+1,J)-VAV(I,J))/DELTAX +(UAV(I,J+1)-UAV(I,J))/DELT
      DEFT(I,J)=(UAVE(I+1,J)-UAVE(I,J))/DELTAX-(VAVE(I,J+1)-VAVE(I,J))/D
      DEF(I,J)=SQRT(DEFS(I,J)**2+DEFT(I,J)**2)
3115
      SCALE=10.**8
      PSIMAX=2.8*SCALE
      DEFMAX=2.*PSIMAX/(DELTAX**2)

      IF(KK.EQ.1) GO TO 3121
      IF(MOD(K,20).EQ.0) GO TO 3121
      GO TO 3126

      PRINT OUT THE DEFORMATION FIELD

3121 DO 3122 J=1,JM
      JS=JMP1-J
      DO 3122 I=1,IM
3122 RESID(I,J)=DEF(I,JS)/DEFMAX
      WRITE(6,3125) ((RESID(I,J),I=1,33),J=1,33)
3125 FORMAT('0','RESID FIELD=DEFORMATION/DEFORMATION MAX',/,
      33(1X,33F4.3,//))
3126 CONTINUE

      AMIN=ALFA
      DO 3130 I=1,IM
      DO 3130 J=1,JM

3130 A(I,J)=AMIN*(1.+999.*DEF(I,J)/DEFMAX)

      IF(KK.GE.0) GO TO 3210

      FX=D/DX(A DU/DX) + D/DY(A DU/DY)
      FY=D/DX(A DV/DX) + D/DY(A DV/DY)

      DO 3205 I=2,IM
      DO 3205 J=2,JM
      FX(I,J)=((A(I,J-1)+A(I,J))/2.)*(U(I+1,J)-U(I,J)) -
      2*((A(I-1,J-1)+A(I-1,J))/2.)*(U(I,J)-U(I-1,J))+
      3*((A(I,J)+A(I-1,J))/2.)*(U(I,J+1)-U(I,J)) -
      4*((A(I,J-1)+A(I-1,J-1))/2.)*(U(I,J)-U(I,J-1))

      FY(I,J)=((A(I,J-1)+A(I,J))/2.)*(V(I+1,J)-V(I,J)) -
      2*((A(I-1,J-1)+A(I-1,J))/2.)*(V(I,J)-V(I-1,J))+
      3*((A(I,J)+A(I-1,J))/2.)*(V(I,J+1)-V(I,J)) -
      4*((A(I,J-1)+A(I-1,J-1))/2.)*(V(I,J)-V(I,J-1))

3205 CONTINUE
      GO TO 3215
3210 CONTINUE
      FX(I,J)=((A(I,J-1)+A(I,J))/2.)*((DEFT(I,J)+DEFT(I,J-1))/2.)-
      2*((A(I-1,J-1)+A(I-1,J))/2.)*((DEFT(I-1,J)+DEFT(I-1,J-1))/2.)+
      3*((A(I,J)+A(I-1,J))/2.)*((DEFS(I,J)+DEFS(I-1,J))/2.)-
      4*((A(I,J-1)+A(I-1,J-1))/2.)*((DEFS(I,J)+DEFS(I-1,J-1))/2.)*DELTAX

      FY(I,J)=((A(I,J-1)+A(I,J))/2.)*((DEFS(I,J)+DEFS(I,J-1))/2.)-
      2*((A(I-1,J-1)+A(I-1,J))/2.)*((DEFS(I-1,J)+DEFS(I-1,J-1))/2.)+
      3*((A(I,J)+A(I-1,J))/2.)*((DEFT(I,J)+DEFT(I-1,J))/2.)-
      4*((A(I,J-1)+A(I-1,J-1))/2.)*((DEFT(I,J)+DEFT(I-1,J-1))/2.)*DELTAX

3215 CONTINUE

      CALCULATE THE CURL OF THE FRICTION FORCE, DEFINED ON THE GRID
      INTERIOR(31,31)
      CURL F = CFY/DX - DFX/DY

      DO 1210 I=3,IM
      DO 1210 J=3,JM
      CURLF=((FY(I,J)+FY(I,J-1))/2. - (FY(I-1,J)+FY(I-1,J-1))/2.)/DELTAX
      -((FX(I-1,J)+FX(I,J))/2. - (FX(I-1,J-1)+FX(I,J-1))/2.)/DELTAY
      F1(I-1,J-1)=CURLF +F1(I-1,J-1)
1210 CONTINUE

      DO 150 I=1,IMM1

```



```

      DO 150 J=1,JMM1
      AA=PSI(I+1,J+1)+ PSI(I+1,J)
      BB=PSI(I,J+1)+PSI(I,J)
      CC=PSI(I+1,J+1)+PSI(I,J+1)
      DD=PSI(I+1,J)+PSI(I,J)
      EE=2.0*DELTA X
      UT(I,J)=0.
      VT(I,J)=0.
      V(I,J)=(AA/EE)-(BB/EE)
150    U(I,J)=((DD/EE)-(CC/EE))
C
C      EASTWARD MASS FLUX
C
      DO 400 I=1,IMM1
      FX(I,1)=U(I,1)
      DO 300 J=2,JMM1
300    FX(I,J)=0.5*(U(I,J)+U(I,J-1))
400    FX(I,JM)=U(I,JMM1)
C
C      NORTHWARD MASS FLUX
C
      DO 600 J=1,JMM1
      FY(1,J)=V(1,J)
      DO 500 I=2,IMM1
500    FY(I,J)=0.5*(V(I,J)+ V(I-1,J))
600    FY(IM,J)=V(IMM1,J)
C
C      EASTWARD ADVECTION OF MOMENTUM V=(FX,FY)
C
      FACT=0.125
      DO 800 I=2,IMM1
      IM1=I-1
      DO 700 J=1,JM
700    GX(I,J)=FX(I,J)+FX(IM1,J)
      DO 800 J=1,JMM1
      FLUX=FACT*(GX(I,J)+GX(I,J+1))
      UFLUX=(U(I,J)+U(IM1,J))*FLUX
      UT(I,J)=UT(I,J)+UFLUX
      UT(IM1,J)=UT(IM1,J)-UFLUX
      VFLUX=(V(I,J)+V(IM1,J))*FLUX
      VT(I,J)=VT(I,J)+VFLUX
800    VT(IM1,J)=VT(IM1,J)-VFLUX
C
C      NORTHWARD ADVECTION OF MOMENTUM (D/DY(VU)+D/DY(VV))
C
      DO 1000 J=2,JMM1
      JM1=J-1
      DO 900 I=1,IM
900    GY(I,J)=FY(I,JM1)+FY(I,J)
      DO 1000 I=1,IMM1
      IP1=I+1
      FLUX=(GY(I,J)+GY(IP1,J))*FACT
      UFLUX=(U(I,J)+U(I,JM1))*FLUX
      UT(I,J)=UT(I,J)+UFLUX
      UT(I,JM1)=UT(I,JM1)-UFLUX
      VFLUX=(V(I,J)+V(I,JM1))*FLUX
      VT(I,J)=VT(I,J)+VFLUX
1000   VT(I,JM1)=VT(I,JM1)-VFLUX
C
C      CURL OF ADVECTION TERMS
C
      DO 190 I=2,IMM1
      DO 190 J=2,JMM1
      AAA=(VT(I,J)+VT(I,J-1))/2.
      BBB=(VT(I-1,J)+VT(I-1,J-1))/2.
      CCC=(UT(I,J)+UT(I-1,J))/2.
      DDD=(UT(I,J-1)+UT(I-1,J-1))/2.
      DELVX= AAA - BBB
      DELUY= CCC - DDD
190    F1(I,J)= F1(I,J)+ DELVX - DELUY
C
C      SET UP FOR SOLVER (DPSIDT=0 ON BOUNDARIES)
C
      DO 2000 J=2,JMM1
      DO 2000 I=2,IMM1
2000   DPSIDT(I,J)=-F1(I,J)
      RETURN
      END

```



```

C      SUBROUTINE SOLVER(B,M,N,DELTAX,DELTAY)
C      FAULKNER DECK 90
C      PCLAND SWEET'S POISSON SOLVER FOR A RECTANGLE
C      REVISED AUG 1974 FOR PROF ROBERT HANEY
C
C      THIS SUBROUTINE SOLVES THE EQUATION LAPLACIAN(Q) = F(I,J), AND RETURNS
C      THE SOLUTION IN B(I,J).
C      B = B(M+1,N+1), WHERE N = A POWER OF TWO.
C      B = -F*DELTAY**2 (UNITS OF Q) ON INTERIOR POINTS.
C      B = SPECIFIED VALUES OF Q ON BOUNDARIES.
C      LAPLACIAN(Q) = 5-POINT DIAMOND APPROX.
C
C      DIMENSION B(33,33), P(33), TWOCOS(33), RECIP(32)
C
C      MM1=M-1
C      NM1=N-1
C      MP1=M+1
C      NP1=N+1
C
C      THIS SECTION GENERATES THE ROOTS OF THE POLYNOMIALS TO BE USED
C      FOR THE REDUCTION AND SOLUTION
C
C      LO = N/2
C      TWOCOS(LO) = 0.
110  L = LO/2
C      TWOCOS(L) = SQRT(2.0 + TWOCOS(LO))
C      LO = L
120  TWOCOS(N-L) = -TWOCOS(L)
C      L = L + 2*LO
C      IF ((2*L/N)*(2*LO-3)) 140,130,110
130  TWOCOS(L) = (TWOCOS(L+LO) + TWOCOS(L-LO))/TWOCOS(LO)
C      GO TO 120
140  CONTINUE
C
C      S = (DELTAX/DELTAY)**2
C      LO = N/2
C      JU = N
C      IU = M-1
C      MM2 = M - 2
C      JUM1 = JU - 1
C      P(N) = 0.
C
C      RIGHT HAND SIDE IS MULTIPLIED BY DELTAY**2, NOW ADD THE PROPER MULTIPLI
C      OF THE UPPER AND LOWER BOUNDARY DATA. THE SIDE BOUNDARY DATA IS
C      ENTERED INTO THE CALCULATION DURING THE REDUCTION.
C
C      DO 200 J=2,JU
C      B(2,J) = B(2,J) + B(1,J)/S
200  B(M,J) = B(M,J) + B(M+1,J)/S
C
C      START REDUCTION
C
C      ID = 1
C      MODE = 2
220  LI = 2*LO
C      IPHASE = 2*MODE - LI/N
C      JD = N/LI
C      JH = N/(2*LI)
C      JT = JD + JH
C      JI = 2*JD
C      JO = JD*MODE + 1
300  DO 750 J=JC,JU,JI
C
C      IPHASE = 3 FOR THE INITIAL STEP OF THE REDUCTION
C      = 4 FOR THE REMAINING STEPS OF THE REDUCTION
C      = 2 FOR THE FIRST STEPS OF THE SOLUTION
C      = 1 FOR THE LAST STEP OF THE SOLUTION BEFORE EXITING
C
C      GO TO (370,350,330,310),IPHASE
C
C      ACCORDING TO IPHASE SET UP PROPER RIGHT HAND SIDE (P ARRAY) AND
C      AMOUNT TO BE ADDED (J-TH COLUMN OF B ARRAY) TO THE SOLUTION OF
C      A CERTAIN SET OF TRIDIAGONAL SYSTEMS

```



```

C
310 DO 320 I=2,M
    PI = B(I,J) - B(I,J-JT) - B(I,J+JT)
    B(I,J) = B(I,J) - B(I,J-JH) - B(I,J+JH) + B(I,J-JD) + B(I,J+JD)
320 P(I-1) = B(I,J) + PI
    GO TO 400
330 DO 340 I=2,M
    P(I-1) = 2.*B(I,J)
340 B(I,J) = B(I,J+1) + B(I,J-1)
    GO TO 400
350 DO 360 I=2,M
    P(I-1) = B(I,J) + B(I,J-JD) + B(I,J+JD)
360 B(I,J) = (B(I,J) - B(I,J-JH) - B(I,J+JH))/2.
    GO TO 400
370 DO 380 I=2,M
    P(I-1) = B(I,J) + B(I,J-1) + B(I,J+1)
380 B(I,J) = 0.

C
C      SOLVE A TRIDIAGONAL SYSTEM WHOSE COEFFICIENT MATRIX HAS THE FORM
C      TRIDIAG(-1,2 + S*(2 - TWOCOS(L)), -1) AND RIGHT HAND SIDE IN
C      P ARRAY. SOLUTION IS BY GAUSS ELIMINATION.
400 DO 700 L=L0,N,LI
    A = 2. + S*(2. - TWOCOS(L))
    RECIP(IU) = -1./A
    P(IU) = P(IU)*S/A
    DO 500 IP=2,MM2
        I = M - IP
        RECIP(I) = -1./(A+RECIP(I+1))
500    P(I) = (S*P(I) + P(I+1))/(A+RECIP(I+1))
        P(1) = (S*P(1) + P(2))/(A+RECIP(2))
    DO 600 I=2,IU
        P(I) = P(I) - RECIP(I)*P(I-1)
600    CONTINUE
    DO 750 I=2,M
        B(I,J) = B(I,J) + P(I-1)
750    GO TO (900,850,800,800), IPHASE
800    LO = LO/2
        IF (LO.EQ. 1) MODE = 1
        GO TO 220
840    IF (LO.GT.1) GO TO 220
850    LO = 2*LO
        IF (LO.LT. N) GO TO 220
900    CONTINUE
    RETURN
    END

```


LIST OF REFERENCES

1. Buneman, O., 1969: "A Compact Non-iterative Poisson Solver," Stanford University Institute for Plasma Research, Report 294.
2. Haney, R.L., 1974: "A Numerical Study of the Response of an Idealized Ocean to Large-Scale Surface Heat and Momentum Flux," Journal of Physical Oceanography, Vol. 4, No. 2, pp. 145-167.
3. Leith, C.E., 1968: "Two Dimensional Eddy Viscosity Coefficients," Technical Report of the Japan Meteorological Agency, No. 67, I-41 - I-44.
4. Kraichnan, R., 1967: "Inertial Ranges in Two-Dimensional Turbulence," Physics of Fluids, pp.1417-1423.
5. Matsuno, T., 1966: "Numerical Integration of the Primitive Equations by a Simulated Backward Difference Method," Journal of Meteorological Society of Japan, 44, pp. 76-84.
6. Miyakoda, K., "Contribution to the NWP - Computation with Finite Difference," Collected Meteorological Papers, Vol. 12, No. 1, Geophysical Institute, Tokyo University, Japan, June 1962.
7. Munk, W.H., "On the Wind-Driven Ocean Circulation," Journal of Meteorology, 7, pp. 79-93, 1950.
8. Smagorinsky, J., "General Circulation Experiments with the Primitive Equations," Monthly Weather Review, Vol. 91, No. 3, pp. 99-154, 1963.
9. Sweet, R., "A Direct Method for Solving Poisson's Equation," NCAR Report No. 22, National Center for Atmospheric Research, Boulder, Colorado, 1972.
10. Takano, K., "Relationship Between the Grid Size and the Coefficient of Lateral Eddy Viscosity in the Finite Difference Computation of the Linear Vorticity Equation in the Ocean," Journal of Oceanographical Society of Japan, (In Press), 1975.

INITIAL DISTRIBUTION LIST

	No. Copies
1. Defense Documentation Center Cameron Station Alexandria, Virginia 22314	2
2. Library (Code 0212) NPS Monterey, California 93940	2
3. Professor R. L. Haney Code 51 Hy	3
4. LCDR J. M. Wright, USN OinC, NWSED USNAS Cubi Pt, Box 63 FPO San Francisco 96654	5
5. Professor G. J. Haltiner Code 51 Ha	1
6. Meteorology Department Code 51 Library	1
7. Oceanography Department Code 58 Library	1
8. Naval Oceanographic Office Library (Code 3330) Washington, D.C. 20373	1
9. Commander, Naval Weather Service Command Naval Weather Service Headquarters Washington Navy Yard Washington, D.C. 20390	1
10. Fleet Numerical Weather Central NPS Monterey, California 93940	1
11. Professor K. L. Davidson Code 51 Da	1
12. Dr. W. L. Gates Physical Science Department Rand Corporation 1700 Main Street Santa Monica, California 90406	1

160787

Thesis

W9135 Wright

c.1

A numerical study of
an idealized ocean us-
ing non linear lateral
eddy viscosity coef-
ficients.

160787

Thesis

W9135 Wright

c.1

A numerical study of
an idealized ocean us-
ing non linear lateral
eddy viscosity coef-
ficients.

thesW9135

A numerical study of an idealized ocean



3 2768 001 90660 5

DUDLEY KNOX LIBRARY